JOURNAL OF GEOPHYSICAL RESEARCH, VOL. 113, F03001, doi:10.1029/2007JF000898, 2008

Long-term morphodynamic evolution and energy dissipation in a coastal plain, tidal embayment

M. van der Wegen,[1] Zheng Bing Wang,[2,3] H. H. G. Savenije,[1,4] and J. A. Roelvink[1,2]

Received 29 August 2007; revised 27 February 2008; accepted 31 March 2008; published 8 July 2008.

[1] The morphodynamic system in alluvial, coastal plain estuaries is complex and characterized by various timescales and spatial scales. The current research aims to investigate the interaction between these different scales as well as the estuarine morphodynamic evolution. Use is made of a process-based, numerical model describing 2-D shallow water equations and a straightforward formulation of the sediment transport and the bed level update. This was done for an embayment with a length of 80 km on a timescale of 3200 years, with and without bank erosion effects. Special emphasis is put on analyzing the results in terms of energy dissipation. Model results show that the basins under consideration evolve toward a state of less morphodynamic activity, which is reflected by (among others) relatively stable morphologic patterns and decreasing deepening and widening of the basins. Closer analysis of the tidal wave shows standing wave behavior with resonant characteristics. Under these conditions, results suggest that the basins aim for a balance between the effect of storage and the effect of fluctuating water level on wave celerity with a negligible effect of friction. Evaluating the model results in terms of energy dissipation reflects the major processes and their timescales (pattern formation, widening, and deepening). On the longer term the basin-wide energy dissipation decreases at a decreasingly lower rate and becomes more uniformly distributed along the basin. Analysis by an entropy-based approach suggests that the forced geometry of the configurations prevents the basins from evolving toward a most probable state.

Citation: van der Wegen, M., Z. B. Wang, H. H. G. Savenije, and J. A. Roelvink (2008), Long-term morphodynamic evolution and energy dissipation in a coastal plain, tidal embayment, *J. Geophys. Res.*, *113*, F03001, doi:10.1029/2007JF000898.

1. Introduction

[2] Estuaries can be defined as the area where fresh river water meets salt seawater. From an environmental point of view these are highly valuable areas. Fresh and salt-water ecosystems coexist and interact with each other. The channel-shoal system of the estuarine bathymetry forms an environment that is tidally renewed with water and nutrients.

[3] Because of the rich ecosystem and strategic location, estuaries have been subject to human settlement. As a result in many estuaries there is a strong impact of human interference. Examples are the construction of groins and dredging of access channels to ports. The morphodynamic system and the related ecosystems are thus artificially disturbed. Further, and on the longer term, sea level rise influences long-term behavior of the morphodynamic system and its impact on the related ecology.

1.1. Morphodynamic Equilibrium

[4] The concept of "morphodynamic equilibrium" refers to a certain natural and steady state of the estuarine bathymetry. This state may even be dynamic in the sense of regular or cyclic migration of shoals and channels and is subject to processes of different spatial scales and timescales interacting with each other in a process of continuous and dynamic feedback [*De Vriend*, 1996]. This implies that equilibrium characteristics are difficult to assess, especially concerning more geological timescales of centuries or millennia. The current research addresses the existence of assumed morphodynamic equilibrium and its related characteristics for a tidal embayment.

[5] Generation and development of channel-shoal patterns have been studied extensively. *Reynolds* [1887] already investigated in laboratory flumes "the action of water to arrange loose granular material over which it may be flowing." More recent examples of numerical approaches to the phenomenon are the investigations by *Schuttelaars and de Swart* [1999], *Seminara and Tubino* [2001], *Schramkowski et al.* [2002], and *van Leeuwen and de Swart* [2004] describing initial channel-shoal formation in highly schematized tidal environments. *Schramkowski et al.* [2004], *Hibma et al.* [2003a, 2003b], *van der Wegen et al.* [2006, 2007], and *van der Wegen and Roelvink* [2008] extended the research to

[1]UNESCO-IHE Institute for Water Education, Delft, Netherlands.
[2]Deltares, Delft, Netherlands.
[3]Hydraulic Engineering Section, Civil Engineering and Geosciences Faculty, Delft University of Technology, Delft, Netherlands.
[4]Water Resources Section, Civil Engineering and Geosciences Faculty, Delft University of Technology, Delft, Netherlands.

0148-0227/08/2007JF000898$09.00

the domain where the bed forms significantly start to influence the hydrodynamic behavior of the system, including the feedback to the morphodynamics.

[6] On an embayment length scale, 1-D model research [*van Dongeren and de Vriend*, 1994; *Schuttelaars and de Swart*, 1996, 2000; *Lanzoni and Seminara*, 2002] led to equilibrium conditions of the longitudinal profile. *Van der Wegen and Roelvink* [2008] investigated pattern formation, the development of the longitudinal profile and their interaction in a 2-D tidal domain. On the timescales considered (~1000 years), they found a relatively stable channel-shoal pattern and a continuously developing longitudinal profile. The existence of two distinct timescales was also found by *Tambroni et al.* [2005] on the basis of laboratory tests. In his mobile bed physical scale models *Reynolds* [1887] also observed a certain steadiness in the development of the channel-shoal system, although he did not report on ongoing development of the longitudinal profile.

1.2. Criteria for Equilibrium

[7] This raises the question in what kind of terms an eventual equilibrium could be defined. *Marciano et al.* [2005] showed that channel structures generated by a 2-D process-based model in a highly schematized tidal environment (similar to the model described in this article) obeyed both Horton's law for drainage network composition [*Horton*, 1945] and observations in the tidal environment of the Waddenzee, the Netherlands. Nevertheless, they recognized that Horton's law cannot discriminate underlying processes and distinct network structures [*Kirchner*, 1993]. *Rinaldo et al.* [1999a, 1999b] and *Feola et al.* [2005] tested different relationships between hydrodynamic properties and morphological conditions for different tidal basin networks and conclude that many geomorphic relationships, that are valid within fluvial conditions, are site specific and do not hold across ranges of scales found in natural tidal networks.

[8] Although the assumed presence of equilibrium is not reflected in several geomorphic relationships stemming from fluvial networks, different other criteria and dominant relationships for estuarine morphodynamic equilibrium are suggested in literature, i.e., and among others, between tidal prism and cross section [*Jarrett*, 1976], an equal duration of ebb and flood [*Dronkers*, 1998], the relation between the M2 and M4 tidal constituents [*Friedrichs and Aubrey*, 1988], the interactions of M2, M4, and M6 tidal constituents [*Van de Kreeke and Robaczewska*, 1993] and the hypsometric characteristics of the estuary [*Boon and Byrne*, 1981]. Further, the impact of the time lag between maximum velocities and maximum water levels has been reported to be a factor of significance [*Ahnert*, 1960; *Friedrichs and Aubrey*, 1988; *Jay*, 1991; *Savenije*, 2001; *Savenije and Veling*, 2005; *Prandle*, 2003]. *Lanzoni and Seminara* [2002], *Prandle* [2003], *Savenije* [2001], *Savenije and Veling* [2005], and *Toffolon et al.* [2006] stress the importance of a landward exponentially decaying cross section for the existence of equilibrium conditions. The importance of the basin length is stressed by *Schuttelaars and de Swart* [2000], *Toffolon et al.* [2006], and *Savenije* [2005].

[9] The above mentioned research on equilibrium conditions in estuaries has been primarily based on an analysis of results derived from the mass and momentum equations. *Singh et al.* [2003] present an extensive historical overview of theories that derive relationships between hydraulic parameters and the geometry of river flow taking energy considerations as a starting point.

[10] *Rodriguez-Iturbe et al.* [1992] combine the criteria of shear stress and sediment transport in their description of energy dissipation in drainage networks. They show that drainage networks in equilibrium aim at a configuration with a minimum of energy dissipation leading to fractal, tree like networks. They base their findings on three principles, i. e., (1) the principle of minimum energy dissipation in any link of the network (a local optimal condition), (2) the principle of equal energy dissipation per unit area of channel anywhere in the river network (a local optimal condition normalized by the topographical characteristics of the local area), and (3) the principle of minimum energy dissipation in the network as a whole (an optimal arrangement of the elements in the network). They suggest that when the first two principles are obeyed the third principle is met as well.

[11] One of the main issues where river regime theory differs from theory on estuarine flow is that, in case of a river, the discharge is often given by constant upstream catchment characteristics, whereas in estuaries there is a mutual interdependency between discharge and geometry, especially considering larger timescales [see *Savenije*, 2005, p.10]. In order to address this issue *Townend* [1999] and *Townend and Dun* [2000] focused on long-term morphodynamic behavior of an estuarine environment by considering the energy flux instead of the energy head usually applied in river regime theory. They suggest that the system leads to a condition in which the energy distribution along an estuary can be described by an exponential function. Deviations between the energy distribution function found in real estaries and the model outcomes are attributed to impact of river discharge, sediment availability, geological characteristics and the impact of man made works (i.e., training works).

1.3. Aim of the Study

[12] The aim of the current research is to investigate the characteristics of 2-D morphodynamic evolution of a coastal plain type of estuary with special emphasis on analyzing the model results in terms of energy dissipation. Use will be made of a process-based, 2-D model describing detailed hydrodynamic and sediment transport processes on both the scale of pattern formation and the total embayment. For an evaluation of the evolution toward equilibrium the method suggested by *Rodriguez-Iturbe et al.* [1992] will be applied. Among other methods that describe evolution and equilibrium, this description was chosen because it includes both the shear stress and the sediment transport criteria for morphodynamic equilibrium.

[13] Two different schematized model configurations will be investigated, i.e., a configuration allowing only deepening of the profile in a rectangular embayment with fixed banks similar to that of *van der Wegen and Roelvink* [2008] (referred to in the following as FBC) and a configuration allowing both deepening and widening of a rectangular embayment by allowing bank erosion (EBC). The EBC was chosen to investigate the behavior of the system allowing adaptation of geometry.

[14] First, we address the governing equations that describe the tidal hydrodynamic and morphodynamic processes. Further, an analysis of the model results will be made

in terms of energy dissipation. Finally, validation of the results is made against the Western Scheldt estuary in the Netherlands and comparison is made to equilibrium conditions suggested by an entropy based approach.

2. Model Description

[15] *Lesser et al.* [2004] and *van der Wegen and Roelvink* [2008] extensively describe the numerical model applied in this research, but it is repeated here briefly for reasons of clarity.

2.1. Hydrodynamics

[16] The hydrodynamic model is unsteady and two-dimensional and is based on the set of shallow water equations. Neglecting the influence of density differences, wind and waves, the two dimensional continuity and the momentum equations read as follows:

$$\frac{\partial \zeta}{\partial t} + \frac{\partial h\overline{u}}{\partial x} + \frac{\partial h\overline{v}}{\partial y} = 0, \tag{1}$$

$$\frac{\partial \overline{u}}{\partial t} + \overline{u}\frac{\partial \overline{u}}{\partial x} + \overline{v}\frac{\partial \overline{u}}{\partial y} + g\frac{\partial \zeta}{\partial x} + c_f\frac{\overline{u}\left|\sqrt{\overline{u}^2+\overline{v}^2}\right|}{h} - \nu\left(\frac{\partial^2 \overline{u}}{\partial x^2} + \frac{\partial^2 \overline{u}}{\partial y^2}\right) = 0, \tag{2}$$

$$\frac{\partial \overline{v}}{\partial t} + \overline{v}\frac{\partial \overline{v}}{\partial y} + \overline{u}\frac{\partial \overline{v}}{\partial x} + g\frac{\partial \zeta}{\partial y} + c_f\frac{\overline{v}\left|\sqrt{\overline{u}^2+\overline{v}^2}\right|}{h} - \nu\left(\frac{\partial^2 \overline{v}}{\partial x^2} + \frac{\partial^2 \overline{v}}{\partial y^2}\right) = 0, \tag{3}$$

with

$$c_f = g\frac{n^2}{\sqrt[3]{h}}, \tag{4}$$

in which

ζ water level with respect to datum (m);
h water depth (m);
$\overline{u}$ depth averaged velocity in x direction (m/s);
$\overline{v}$ depth averaged velocity in y direction (m/s);
g gravitational acceleration (m/s^2);
c_f friction coefficient (dimensionless);
n Manning's coefficient (sm$^{-1/3}$);
ν eddy viscosity (m^2/s).

The Manning's coefficient and eddy viscosity were taken constant with values of 0.026 sm$^{-1/3}$ and 1 m^2/s respectively.

2.2. Morphodynamics

2.2.1. Sediment Transport Formulation

[17] The velocity field obtained by solving the equation of continuity and the momentum equations is used to calculate the sediment transport field. Use is made of the instantaneous total sediment transport formula developed by *Engelund and Hansen* [1967] that relates velocity directly and locally to a sediment transport. The Engelund-Hansen sediment transport formula reads as follows:

$$S = S_b + S_s = \frac{0.05U^5}{\sqrt{g}C^3\Delta^2 D_{50}}, \tag{5}$$

where

S Sediment transport (m^3/ms);
U magnitude of depth averaged flow velocity (m/s);
Δ relative density $(\rho_s - \rho_w)/\rho_w$ (dimensionless);
ρ_s sediment density (kg/m^3);
ρ_w water density (kg/m^3);
C friction parameter defined by $\frac{\sqrt[6]{h}}{n}$ (m$^{1/2}$/s);
n Manning's coefficient (sm$^{-1/3}$);
D_{50} median grain size (m).

The authors chose for this transport formulation (which makes no distinction between suspended load and bed load) for reasons of simplicity. Longitudinal and transverse bed slope effects are taken from research by, respectively, *Bagnold* [1966], *Ikeda* [1982], and *Ikeda and Aseada* [1983] as presented by *Van Rijn* [1993].

[18] Different authors (among others *Groen* [1967], *Lanzoni and Seminara* [2002], *Prandle* [2004], *van Leeuwen and de Swart* [2004], and *Pritchard* [2005]) have pointed to the importance of suspended sediment transport for prediction of equilibrium conditions in a tidal embayment, especially regarding the settling lag effect. However, it is argued that processes of bringing sediment into suspension and settlement of suspensive sediments take place within the grid cells of the current model (100 transverse m by 200 longitudinal m) and do not significantly affect the amount of transported sediments. *Pritchard* [2005] confirms that for relatively large ratios of the tidal timescale to the timescale over which the sediment concentrations respond to changes in erosion and deposition rates, lag effects are small. This holds for the current research with a uniform sediment size of 240 μm. Preliminary calculations with transport formulations including a distinction between suspended load and bed load showed results that are comparable to the results presented in the current research. Finer sediments would increase the settling lag effect and probably induce a net landward transport.

2.2.2. Bed Level Update

[19] Conservation of sediment is described by the following equation representing a balance between the divergence of the sediment transport field and the evolution of the bed level corrected for bed porosity

$$(1-\varepsilon)\frac{\partial z_b}{\partial t} + \frac{\partial S_x}{\partial x} + \frac{\partial S_y}{\partial y} = 0, \tag{6}$$

where

ε bed porosity, default 0.4 (dimensionless);
z_b bed level (m);
S_x sediment transport in x direction (m^3/m/s);
S_y sediment transport in y direction (m^3/m/s).

2.3. Numerical Aspects

2.3.1. Hydrodynamic Model

[20] The numerical scheme applies an orthogonal, staggered grid, where water level points and depth points are colocated in the cell centers and the u and v velocity points are located in the middle of the cell walls. An Alternating Direction Implicit (ADI) method is used to solve the continuity and momentum equations [*Leendertse*, 1987]. The advantage of the ADI method is that the implicitly

integrated water levels and velocities are coupled along grid lines leading to systems of equations with a small bandwidth. *Stelling* [1984] extended the ADI method of *Leendertse* [1987] with a special approach for the horizontal advection terms, namely the splitting of a third-order upwind finite difference scheme for the first derivative into two second-order consistent discretisations: a central discretisation and an upwind discretisation, which are successfully used in both stages of the ADI scheme. The scheme is denoted as the "cyclic method" [*Stelling and Leendertse*, 1991].

2.3.2. Morphodynamics

[21] With respect to the morphodynamic model the following important procedures, slightly deviating from *Lesser et al.* [2004], where followed: (1) the depths in u and v points are taken as the minimum of the surrounding depths in water level points; (2) the velocity vectors applied in the centers are determined by a depth-weighted averaging of the surrounding velocities in u and v points; (3) the sediment transport components in the u and v points are copied from the upstream water level points where the transport is evaluated; (4) the bottom change (in water level points) over half a time step is computed as the net sediment transport into or out of a cell.

2.3.3. Morphodynamic Update

[22] The hydrodynamic behavior has a timescale that is typically 1 to 2 orders of magnitude smaller than the morphodynamic timescale. In terms of numerical modeling this implies that many hydrodynamic calculations need to be performed that have only limited effect on the morphology. It is only after several weeks (i.e., tens of tidal cycles) that the impact on the bed becomes relevant. Morphodynamic calculations would therefore require long and inefficient hydrodynamic calculation time. In order to increase the efficiency of process-based morphodynamic models an approach suggested by *Roelvink* [2006] is applied. In this approach the bed level change calculated every hydrodynamic time step is increased by a morphological factor and results in the bed level used in the next hydrodynamic time step.

[23] The main advantage is that the stability and accuracy of the method are less restrictive than the tidally averaged methods suggested, for example, by *Latteux* [1995] and that the update scheme allows propagation of morphological features during a tide [*Roelvink*, 2006]. The leading guideline to apply the methodology is that bed level changes within one tidal cycle should not exceed 10% of the water depth so that distortion due to the influence of the nonlinear interaction with the hydrodynamics does not become too relevant.

[24] For a model configuration similar to the current configuration *van der Wegen and Roelvink* [2008] carried out an extensive sensitivity analysis concerning the value of the morphological factor (MF). They showed that even MF values of 1000 lead to stable solutions that compared relatively well with results obtained with MF values of 1 and 10. In general terms, higher MF values lead to larger spatial phase shifts and a more diffuse character of the patterns developing. This means that on individual spatial points this may result in large differences, although the patterns themselves are largely maintained.

[25] Sensitivity analysis indicated that a factor of 200 is more appropriate for the current model settings, because of the large impact of the bank erosion effect. This causes relatively high sediment transports and made the basin relatively shallow at the start of the model runs. Both effects resulted in bed level updates that frequently exceeded 10% of the water depth when a morphological factor of 400 was applied.

2.3.4. Dry Cell Erosion and Bank Erosion

[26] The reason for applying a bank erosion algorithm is twofold. First in previous runs, excluding bank erosion, shoals emerged that remained dry during the rest of the run and acted as, unphysical, fixed points of the morphodynamic system. This probably happened because of water levels, dropping from high water at a particular location, were not able to reach the top of the shoal again because of small hydrodynamic adaptations during the tide. A second reason is that the geometry of a tidal basin highly affects the hydrodynamic and morphodynamic behavior. Including bank erosion in the model runs would allow for investigating its impact on emerging basin geometry and hydrodynamic conditions.

[27] Bank erosion is a function of (among others) local shear stresses and sediment properties such as the angle of internal repose and cohesion. Further, just as the deepening process of the bathymetry, the widening process due to bank erosion has its own typical timescale. A particular problem in relation to numerical models is that bank erosion is a process that requires gradual erosion of banks, which often cannot be resolved by the grid of the hydrodynamic model. Research is in progress to describe bank erosion on different timescales and spatial scales. *ASCE Task Committee on Hydraulics, Bank Mechanics, and Modeling of River Width Adjustment* [1998a, 1998b, and references therein] provide an overview of relevant processes and modeling techniques. However, an accurate and validated approach that could be applied in the process-based numerical approach of the current research is not known to the authors.

[28] In our model a relatively simple formulation is applied. Bank erosion is allowed by assigning the erosion that is taking place in a wet cell to the adjacent dry cell. Implicitly this means that sediment is transported from a dry cell to a wet cell so that no bed level change of the wet cell takes place. The procedure continues until the dry cell becomes wet again. The same procedure is applied for cells that become dry during the run. This can be the result of the tidal movement, or the morphological factor which locally may cause high deposition so that wet cells to become dry.

[29] The bank erosion algorithm applied implies that the bank erosion is a direct function of morphodynamic developments taking place under water next to the dry area. The relatively large grid resolution of 100 by 200 m does not cover gradual lateral bank erosion processes. Applying smaller grid cells would describe the process more adequately, in the sense it allows for a more gradual development. Further, it implicitly also assumes that the banks consist of loosely packed sediments, so that soil properties (like, for example, compaction and moisture) or ecological impacts [*Murray et al.*, 2007] are not considered. It is also important that the banks are not defined too high so that the gradient between the bed level in the wet cell and the bed level at the bank does not become higher than the internal angle of repose. Larger gradients introduce steep slopes and would imply that banks are cohesive, which is

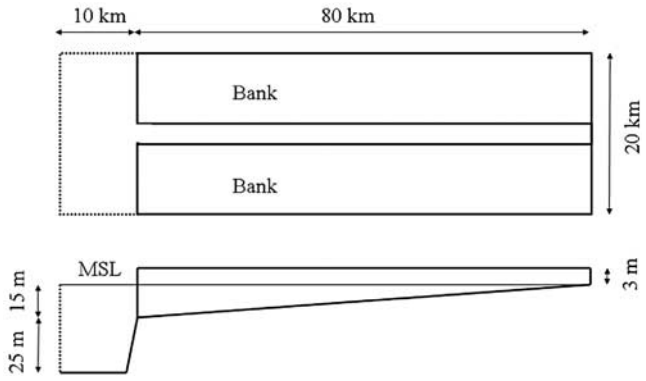

Figure 1. Model configuration. The dotted line represents the seaward boundary.

not the case for the current research. *Roelvink et al.* [2003] validate the method for a short timescale, extreme condition, namely a barrier island breach. More research would be desirable on validation of the bank erosion algorithm behavior on different grid sizes and longer timescales, but this is considered outside the scope of this study.

2.3.5. Drying and Flooding

[30] The intertidal area in the model alternates between wet and dry states during the tidal cycle. The cells that fall dry are removed from the hydrodynamic calculation. When the tide rises and the cells become wet again, they are reactivated. Cells become dry when the water depth decreases below a certain threshold value (0.1 m in this study). This means that the velocity is set to zero. The cell is closed at the side normal to the velocity. When all four velocity points of a cell surrounding a water level point are dry, the cell is excluded from computation. If the water level rises and becomes larger than twice the threshold level, the velocity point is reactivated.

2.4. Model Configuration

[31] The current research is based on an 80 km long rectangular embayment. The reason why this size was chosen is that it resembles the shape of the Western Scheldt estuary in the Netherlands. It can be classified as a coastal plain estuary following the definition of *Pritchard* [1952], with a mesotidal to macrotidal range following the classification by *Hayes* [1975].

[32] *Van der Wegen and Roelvink* [2008] validated a similar model configuration on the basis of data from the Western Scheldt estuary. One of the drawbacks of their approach was that the seaward boundary was located at the mouth of the basin and was prescribed solely by a semidiurnal tide water level fluctuation. Although the model allowed for the generation of overtides within the model domain, describing only a semidiurnal water level fluctuation at the estuary inlet seems inappropriate to model inlet morphodynamics. Therefore, in the current research, the model domain was extended seaward which is shown in Figure 1. In this way, developing overtides within the model domain account for more realistic conditions at the inlet. As a result and because of the sediment exporting character of the basin, this also allowed for the formation of an ebb tidal delta. A closer analysis of the delta characteristics will be the subject of future research.

[33] The boundary condition at the seaward end (i.e., the northern, southern and western parts of the sea boundary) is described by a varying water level with an amplitude of 1.75 m and a period of 12 h. The boundary at the head is closed allowing no transport of water or sediment across the head. This agrees with discharges from the Scheldt River, which are negligible with respect to prevailing tidal discharges in the Western Scheldt. Furthermore, no wind or wave action, density currents or sea level rise were considered.

[34] The width of the FBC is 2.5 km and the initial width of the EBC is 500 m. No transport of water or sediment across the banks is allowed in case of the FBC. The banks at EBC are specified at a level of mean sea level (MSL) + 3.2 m, slightly larger than the maximum observed tidal water levels. This causes only gentle slopes between wet and dry cell bed levels and supports the assumed condition of loosely packed sediment. Preliminary calculations showed that, after some time, lower bank levels lead to major flooding of banks near the head, which resulted in major infilling of the embayment. This extra sediment supply acted as an extra disturbance of the system and increased the adaptation time considerably. Therefore the bank levels where set at a value that would not allow for flooding during the model runs

[35] By running the model in a 1-D mode, *van der Wegen and Roelvink* [2008] showed that a bed level varying from MSL – 34 m at the mouth to MSL at the head resembles a morphodynamically stable profile for an embayment length of 80 km. However, such a deep bed level as a starting point for a 2-D configuration would mean that the 2-D pattern needs a long time (∼millennia) to develop from scratch. A shallower profile is preferred, since an important aspect of the current research is to investigate the impact of pattern formation on the estuarine evolution. Additionally, comparison to the bed level of the Western Scheldt shows a much shallower basin. Therefore, the initial bed level is taken linearly sloping from MSL – 15 m at the mouth toward MSL at the head, so that the channel shoal system can develop within decades. Further, the initial, linear bed level was randomly disturbed by perturbations of maximum 5% of the water depth in order to provoke pattern formation.

3. Results

3.1. Fixed Banks

3.1.1. FBC Pattern Formation and Longitudinal Profile

[36] Figure 2 shows some illustrative output from the model (see Animations 1 and 2).[1] Initially, the perturbations of the initial bed level grow to larger-scale bed forms especially in the area near the head of the basin. The reason why the pattern development takes in that particular area is attributed to the relatively high impact of friction in the shallower part of the basin. There the flow is attracted by the deeper cells that have less friction and which interconnect and evolve into small channels. The shoals in between may even develop into intertidal area. Further in time, bed forms develop slowly toward the mouth, because the flow is disturbed by the pattern developing at the shallower part. This continues until the complete basin is covered by a channel-shoal system after approximately 100 years.

[1] Animation is available in the HTML.

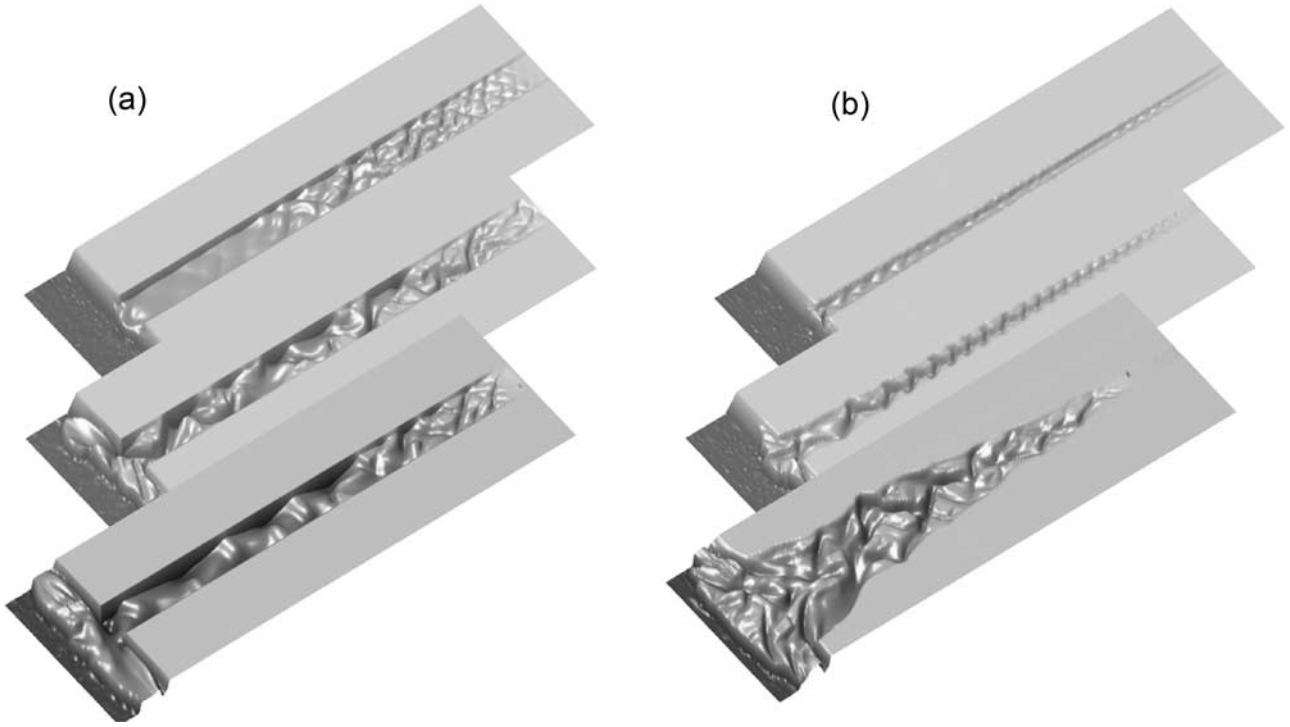

Figure 2. Impression of bathymetry after 25,400 and 3200 years (a) for FBC and (b) for EBC on a distorted scale. See Animations 1 and 2.

[37] At the landward end multiple channels are distributed over the width, whereas in the area from the mouth toward about 60 km landward an alternating bar pattern is apparent. After the first decades, the main characteristics of the channel-shoal system are roughly maintained, such as bar and meander channel length scales and the alternating bar pattern. However, seaward migration of the shoals and small changes in characteristic length scales are observed. These are attributed to the deepening longitudinal profile and its impact on the tidal wave characteristics.

[38] Because of the exporting character of the embayment an ebb tidal delta forms outside the mouth. It is characterized by a shallow wedge toward the mouth which is separated from the banks by two main channels. The channels are alternatively dominant in conveying the main tidal flow and sometimes migrate across the wedge. Detailed analysis of the ebb delta lies not within the scope of this research and will be a subject of future research.

[39] *Van der Wegen and Roelvink* [2008] distinguished two typical scales, which also holds for the current research. One is for the pattern formation with a timescale of decades and a spatial scale of the basin width or the water depth for the shallower parts. The other scale is related to the width averaged longitudinal profile with a timescale in the order of millennia and a spatial scale related to the basin length.

[40] Figure 3a shows that the width averaged longitudinal profile increases to MSL + 2 m at the head within the first decades. The profile at the head remains further relatively constant in time. Near the mouth the longitudinal profile continuously deepens and the profile along the basin becomes concave. This process continues but becomes gradually less pronounced. Comparison of the profiles after 1600 and 3200 years shows only little deepening with

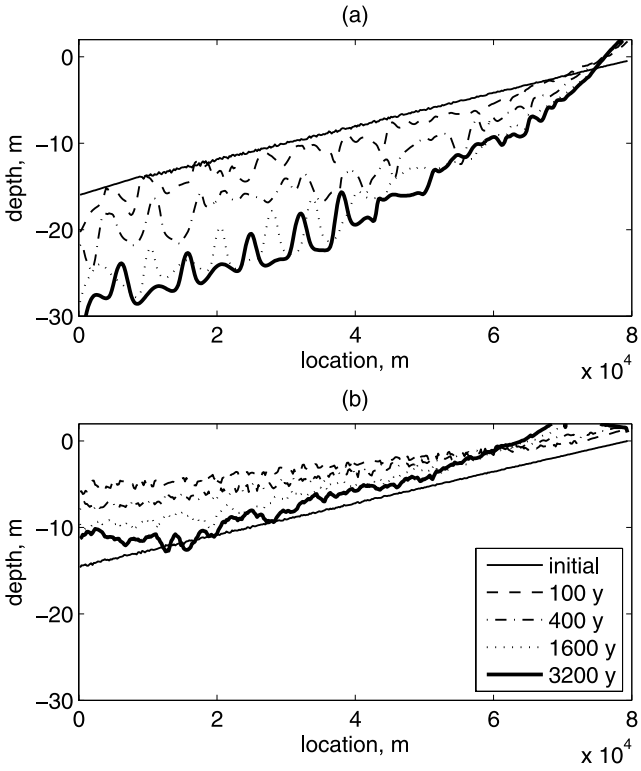

Figure 3. Development of width-averaged longitudinal profile over time (a) for FBC (b) for EBC.

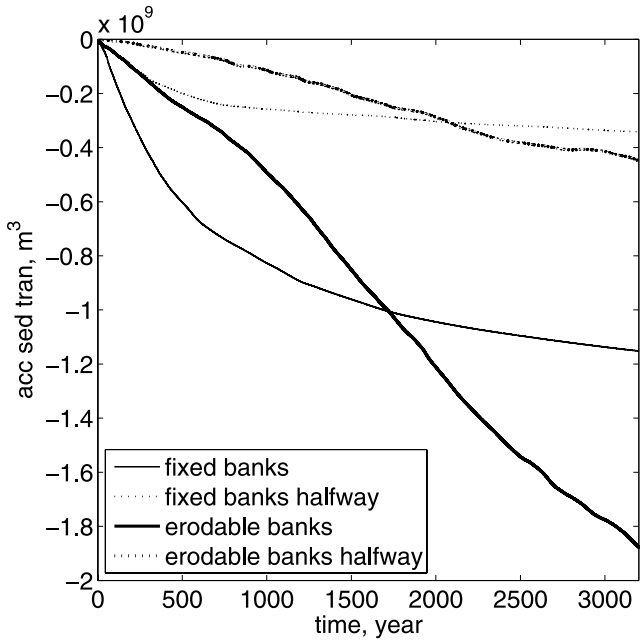

Figure 4. Accumulated sediment transport through basin wide cross section (m^3) over time for FBC (thin lines) and for EBC (thick lines). Solid lines show transport at the mouth, and dashed lines show transport halfway (40 km landward from the mouth).

respect to the deepening compared to the profiles after 100 and 400 years. This is confirmed by considering the accumulated sediment transport over different cross sections along the basin, Figure 4. Halfway along the channel and at the mouth the embayment continuously directs sediments seaward which results in a pronounced ebb tidal delta.

3.1.2. FBC Tidal Amplitudes

[41] Figures 5a and 5b show around low water and high water, respectively, the water levels at the seaward boundary compared to water levels 2 km landward from the mouth for the FBC. Small delays of low water and high water are present because of the 20 km distance the tidal wave needs to travel toward the mouth. Initially, the high water amplitude remains constant and that the low water amplitude increases.

[42] Figures 5a and 5b show, around low water and high water, respectively, the water levels at the seaward boundary. The tidal amplitude was determined by dividing the tidal difference by two. However, the amplitude profile slowly evolves toward an amplitude, which linearly increases from 1.8 m at the mouth to 2.8 m at the basin head after 400 years. The linear amplification and the damping agrees with *Savenije* [2001]. Over the longer term the amplitude decays again although the decay itself becomes less. The amplitude increase is attributed to resonant behavior of the tidal wave. Under shallow water conditions the celerity (c) of the tidal wave can be approximated by $c = \frac{L_{tide}}{T} = \sqrt{gh}$. With a tidal period ($T$) of 12 h, the tidal wavelength (L_{tide}) halfway the embayment (assuming that h = 7.5 m) is approximately 370 km. Resonance

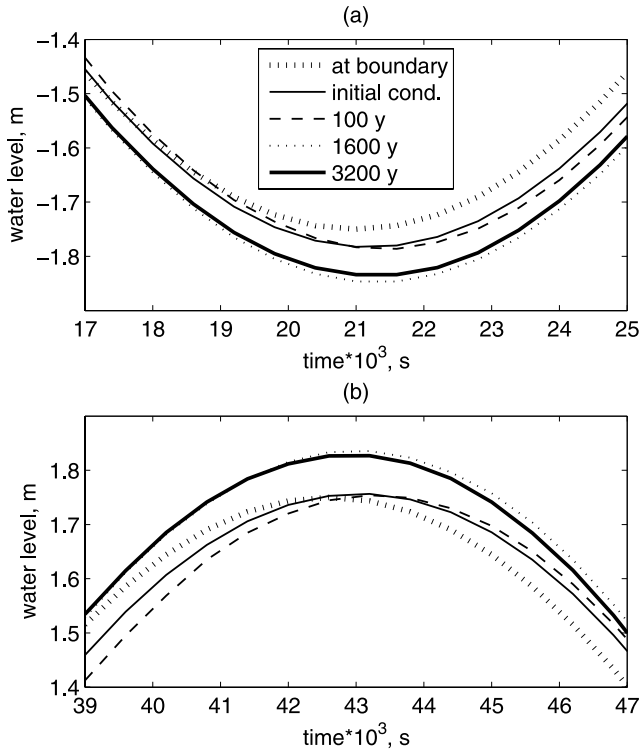

Figure 5. Water level fluctuations in FBC at seaward boundary (thickest line) and 2 km landward from the mouth (other lines) at different points in time (a) near low water and (b) near high water.

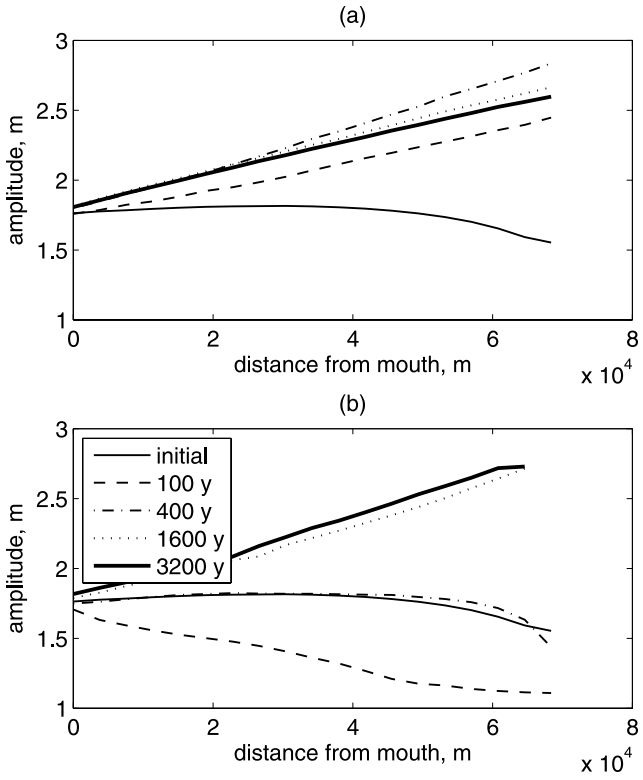

Figure 6. Tidal amplitude (defined by (highest water level − lowest water level)/2) along the basin for different points in time (a) for FBC and (b) for EBC. Data near the head are not shown since this area falls completely dry at relatively low water.

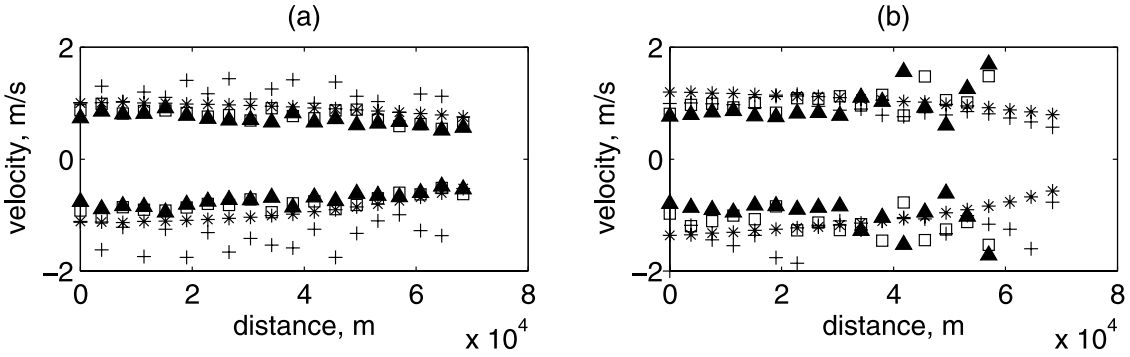

Figure 7. Maximum width averaged ebb (negative values) and flood (positive values) velocities along the basin for different points in time (stars are initial condition, crosses are 100 years, squares are 1600 years, and triangles are 3200 years) (a) for FBC and (b) for EBC. Data near the head are not shown since this area falls completely dry at relatively low water.

will occur for a basin size of $L_{basin} = {}^{n}/_{4}\, L_{tide}$, for $n = 1, 2, 3\ldots$ For n = 1 the embayment length of 80 km is close to a resonant basin size. Hence the estuary belongs to the category of short estuaries that develops a standing wave.

3.1.3. FBC Velocities, Time Lags, and Ebb/Flood Duration

[43] Figure 7a shows the development of maximum flow-width-averaged ebb and flood velocities over time. Initially, ebb flows are larger than flood flows apart from the area near the head. Pattern formation within the first 100 years increases both ebb and flood flows, because the relatively high friction on the shoals stimulates water to flow through the relatively small cross sections of the channels. Over the longer term the velocities decrease again below the initial values because of the deepening of the profile and the difference between ebb and flood velocities disappears.

[44] Figure 8a shows a time lag of about $1/3\pi$ (or about 120 min based on a tidal period (T) of 720 min) between slack water and MSL initially present at the mouth. This time lag increases to $1/2\pi$ over the longer term and for the whole basin, which reflects standing wave conditions. Especially near the head, the time lag between maximum flood and high water shows a more diffusive result, than the time lag for the ebb and low water. This is attributed to the fact that flow-width-averaged values were taken, so that the lag values reflect the impact of the channel-shoal pattern. Results include the complex process of water exchange between flats and channels, which is held responsible for the diffuse results near the head.

[45] Figure 9a shows that ebb and flood duration are similar at the mouth and that ebb (flood) duration is larger (smaller) for the remaining part of the basin, although ebb and flood duration become similar over the longer term. The following section provides a possible physical explanation of the observations. The impact of friction is initially high resulting in a decrease of the tidal amplitude and the tidal velocities along the basin (Figures 6a and 7a, respectively). The relatively small time lag between maximum slack water and MSL (Figure 8a) is initially probably caused by friction. Water levels are lower during ebb than during flood. This means that, especially at the intertidal shoals near the head, the impact of friction is high during ebb and the shoals drain their water slowly toward the channels and prolong ebb (Figure 9a), whereas inundation takes place more rapidly. As a result of the long ebb duration, ebb velocities are relatively low near the head.

[46] Ebb velocities near the mouth are relatively large compared to the flood velocities. The first reason might be the phase lag between the water levels and velocities, which induces a landward Stokes' drift. Since the embayment is closed at one end, higher mean water levels develop toward the head and, as a consequence, a seaward return flow emerges, which enhances ebb velocities. A second reason is related to higher water level gradients during ebb. For a stationary flow through a uniform cross section over a horizontal bed, friction leads to a downstream water level gradient. Although this might be somewhat counterintuitive, as a consequence, continuity requires downstream acceleration of flow. In the current models a similar effect might occur, despite the fact that the flow is not stationary and bed levels are not horizontal. The phenomenon will be more pronounced during ebb flow, because of the lower water levels and the higher impact of friction. Figure 5 shows that, initially, the lowest water levels in the mouth are lower than the low water level at the relatively deep sea boundary. In contrast, this effect is not observed for the high water levels.

[47] Over the longer term, when the profile deepens, the impact of friction becomes less and more energy of the incoming tidal wave reflects against the head. Resonance occurs and standing wave conditions develop, which results in a time lag of about $1/2\pi$ (Figure 8a), and similar water levels during ebb and flood. The Stokes's drift then disappears, ebb and flood velocities become similar (Figure 7a), and ebb and flood duration become equal along the basin (Figure 9a).

3.1.4. FBC Relation to Wave Celerity

[48] On the basis of highly schematized 1-D model results, *Friedrichs and Aubrey* [1988] derived a relationship for morphological equilibrium conditions in short tidal embayments with intertidal area. The relationship is between the ratio of the water volume stored on the shoals and the channel volume (V_s/V_c) and the ratio of the tidal amplitude and the water depth (a/h). *Friedrichs and Aubrey* [1988] suggest that the duration of flood is increased by water storage on intertidal flats and that ebb duration is prolonged by friction, which increases at lower water levels. Further, they mention the effect of water level on tidal wave

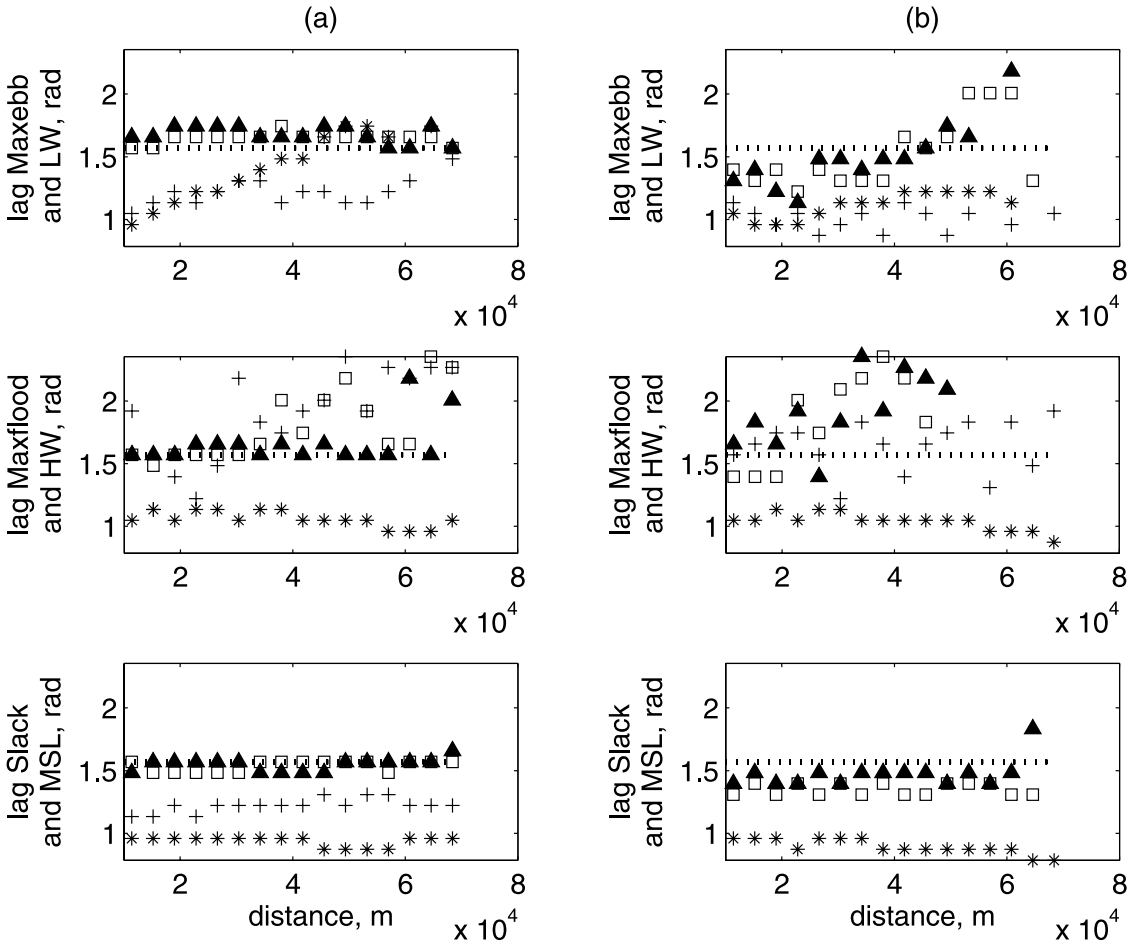

Figure 8. Time lags between maximum flow width averaged ebb velocities, flood velocities, and slack water after high water and high water, low water, and MSL after high water, respectively, along the basin for different points in time (stars are initial condition, crosses are 100 years, squares are 1600 years, and triangles are 3200 years) (a) for FBC and (b) for EBC. Data near the head are not shown since this area falls completely dry at relatively low water. Dashed lines indicate values of $1/2\pi$.

celerity, which becomes smaller at relatively low water levels [*Airy*, 1845] and causes longer ebb duration as well.

[49] *Wang et al.* [1999] combined the schematized model configuration of *Friedrichs and Aubrey* [1988] with the assumption of *Dronkers* [1998] that morphodynamic equilibrium can only be present in case of equal ebb and flood duration. This yields the following equation that resembles the results of *Friedrichs and Aubrey* [1988], at least for $V_s/V_c < 1$, which is the relevant range for the current study

$$\frac{V_s}{V_c} = \frac{8}{3}\frac{\left(\frac{a}{h}\right)^2}{1-\frac{a}{h}}\left(\frac{1+\frac{a}{h}}{1-\frac{a}{h}}\right)\left(\frac{3}{4}+\frac{1}{4}\frac{a}{h}\right)^{-1}. \quad (7)$$

For the current research, the shoal volume was calculated by the maximum volume of water present above intertidal area during a tidal cycle. The channel volume was calculated as the volume of water below MSL and not belonging to intertidal area, see also Figure 10. This was based on the definition by *Friedrichs et al.* [1990]. Further, (a) and (h) were defined locally, which is somewhat different than *Friedrichs and Aubrey* [1988], who define (a) at open sea and (h) as the average water depth in the basin.

[50] Figure 11a shows model results of the (V_s/V_c) and (a/h) relationship. The results were obtained by separated model runs on a constant bathymetry (no morphodynamic updating) at different points in time. Comparison of the initial bed level and the bed level after 100 years shows that the development of intertidal shoals has initially a high impact. The deepening of the profile and the increase of amplitude in later stages (>100 years) lead to a gradual development toward the equilibrium line defined by equation (7) The conditions at the mouth move slowly toward the lower left corner. *Friedrichs and Aubrey* [1988] suggest that the area to the left of the line representing equation (7), can be considered ebb dominant, whereas the area to the right is considered flood dominant. Near the head the model results are in the flood dominant domain, whereas toward the mouth they approach the equilibrium condition defined by equation (7). Closer analysis of ebb and flood duration along the basin presented in Figure 9a leads to similar conclusions. Initially, ebb duration is longer than flood duration, especially in the landward part of the basin. Over the longer term the ebb and flood duration become similar along the basin.

[51] *Friedrichs and Aubrey* [1988] suggest that the higher friction during the ebb and that fact that the tidal wave

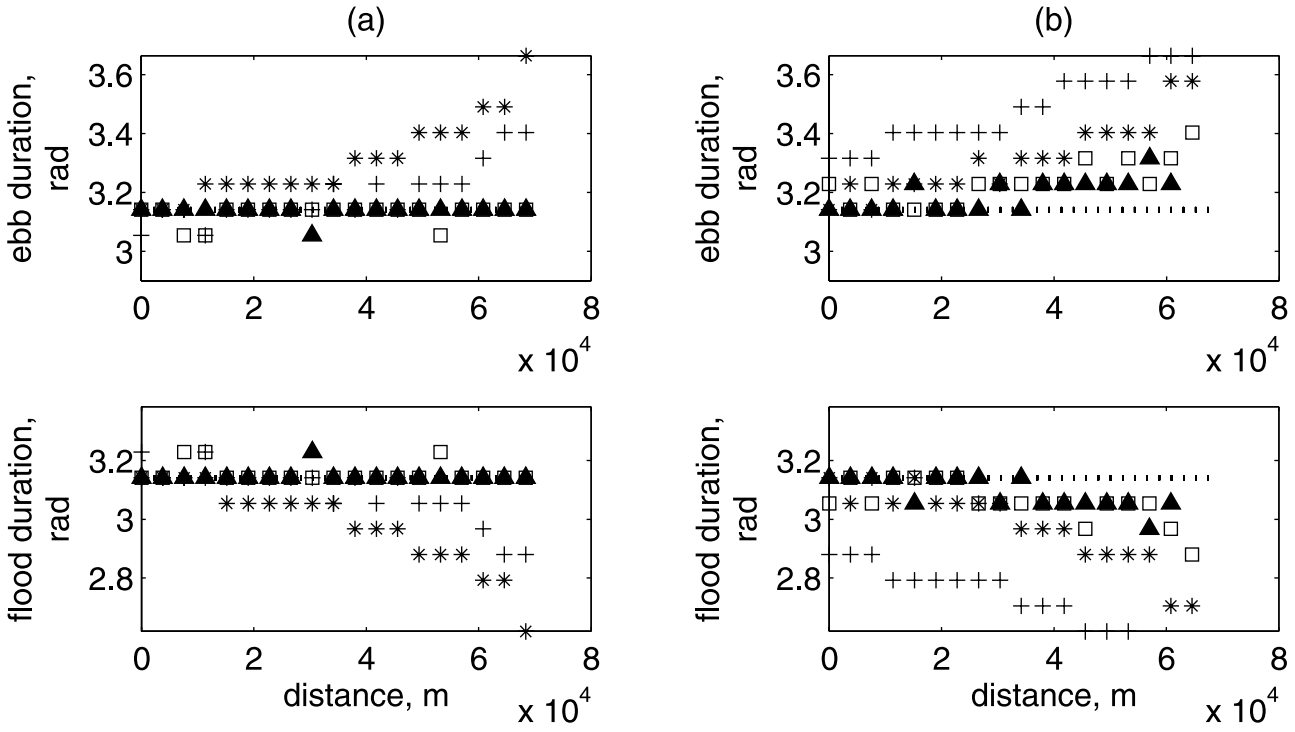

Figure 9. Duration of ebb and flood along the basin for different points in time (stars are initial condition, crosses are 100 years, squares are 1600 years, and triangles are 3200 years) based on width-averaged values for the velocities and water levels (a) for FBC and (b) for EBC. Data near the head are not shown since this area falls completely dry at relatively low water. Results are at discrete intervals because they are based on output generated at 10 min intervals. Dashed lines indicate values of π.

celerity is smaller at relatively low water levels both account for a faster propagating flood wave, a shorter flood period, higher flood velocities and, as a consequence, an importing basin. It is, however, remarkable that the evolution of the current basin is from the flood dominant domain in Figure 11a toward a form that reflects morphodynamic equilibrium, which is achieved by a continuously exporting basin (Figure 4a). Apparently, the effect of water storage on intertidal flats and the effects of friction and water depth on wave propagation are not sufficient to explain the evolution of the current model configuration.

[52] A possible explanation can be provided in terms of the Stokes' drift that results from flood flows taking place at higher water levels than ebb flows. In an infinitely long basin the Stokes' drift would thus transport water in the direction of the tidal wave propagation. However, for a closed embayment, mass continuity requires that the drift is counteracted by a seaward directed return flow. This return flow leads to higher ebb velocities (Figure 7a) enhancing the ebb dominant and exporting character of the basin.

[53] On the basis of the presented results one may assume that a form of equilibrium is reached after 3200 years reflecting an equilibrium between the effect of storage (V_s/V_c) and deviations in wave celerity at higher or lower water levels ($c = \sqrt{g(h \pm a)}$). At that point in time, tidal water motion is characterized by a standing wave with maximum ebb and flood velocities taking place at MSL and with approximately similar values and distributions along the basin (Figure 7a). The effect of friction is equal

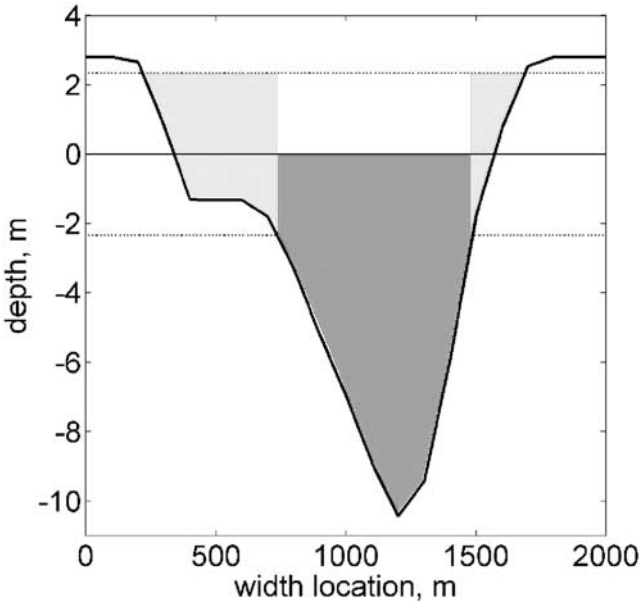

Figure 10. Definition sketch of EBC cross section (thick line) at 50 km from the mouth, including high water and low water (dotted lines) and MSL (thin line). Dark-shaded area represents channel volume (V_c). Light-shaded area represents shoal volume (V_s).

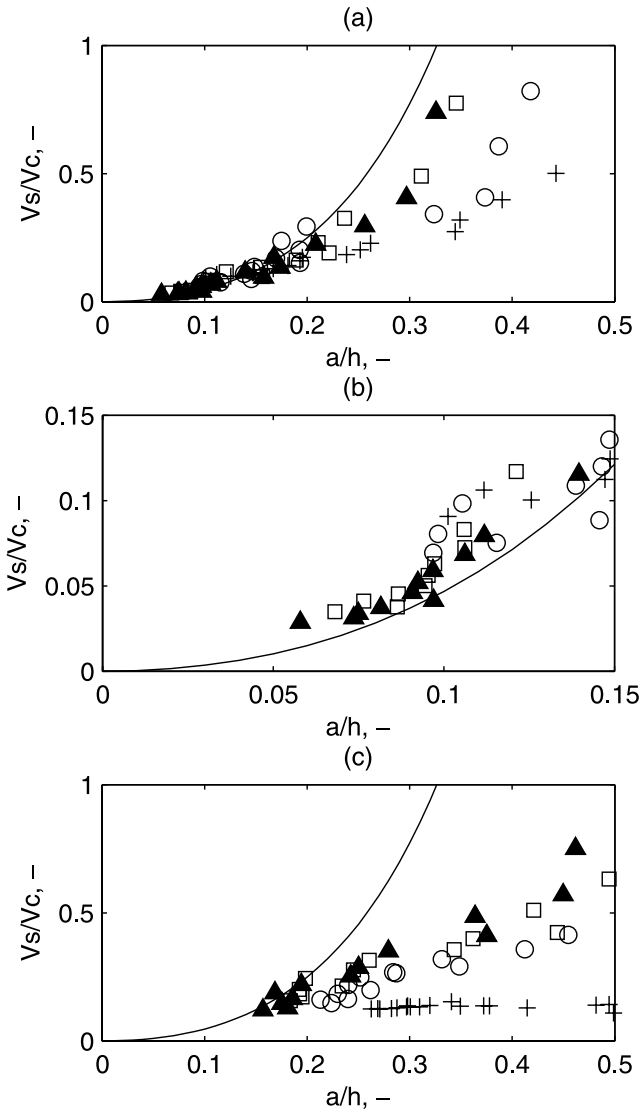

Figure 11. Relation of (a/h) and (V_s/V_c) ratios for model results at different point in time (crosses are 100 years, circles are 400 years, squares are 1600 years, and triangles are 3200 years) and results by equation (7) represented by the line (a) for FBC (b) for the detail of Figure 11a, and (c) for EBC.

during ebb and flood and may be neglected for its impact on wave propagation for this specific configuration.

[54] Despite the suggested equilibrium conditions, Figure 4a shows a continuing sediment export from the basin even after 3200 years. A probable explanation for this is that minor nonlinear processes still have an important long-term effect on the basins' morphodynamics. The nonlinearities originate from the mass balance equation, both the advection term and the friction term in the momentum equation [*Parker*, 1991] and the sediment transport formulation. An example of latter is the effect of the interaction between the M2, M4, and M6 tidal constituents on the bed load transport suggested by *van de Kreeke and Robaczewska* [1993]. It is highly questionable whether the overtides and the associated tide residual transports will finally disappear.

3.2. Eroding Banks

3.2.1. EBC Pattern Formation and Widening

[55] The major difference between the EBC and the FBC is the widening of the basin (Figure 12a) and the resulting large supply of sediments from the banks. Within the first century the EBC embayment is therefore subject to sedimentation resulting in an initially relatively shallow longitudinal profile (Figure 3; see Animations 1 and 2). Over the longer term, the basin deepens again because the supply of sediment from the banks becomes smaller than the exporting capacity of the basin. At the same time, a small part of the sediment is transported toward the head where some sedimentation occurs just as in the FBC. Major sedimentation at the head takes place between 400 and 1600 years, which shortens the basin considerably. The exporting process after 3200 years is more pronounced than in the FBC, which is reflected in a higher (gradient of the) accumulated sediment transport after 3200 years (Figure 4) and the continuous deepening (Figure 3b) and widening (Figure 12a) processes.

[56] The widening of the basin appears to be strongly related to channel bends touching and eroding the banks. Because of slow migration of the channel bends and the development of new channels, widening takes place along the complete basin. Initially, there is a pronounced and regular alternating bar pattern present in the basin. After approximately 100 years, especially near the mouth, the main sinusoidal channel grows in amplitude, width and length. Later, after about 1000 years, the main channel breaks up and smaller channels are forming, growing and merging with each other on its remnants. After 3200 years one could distinguish a major channel again having an amplitude of the basin width and a length scale of about half the basin. Figure 2b shows a distorted network of major channels, old channels, new small channels and smaller crosscut channels. The dynamics of the system is still higher than the FBC, and the widening process shows little decline over the long term. In contrast, *van der Wegen et al.* [2007] show that the rate of widening for a 20 km long basin decreases considerably after a period of about 4000 years.

3.2.2. EBC Tidal Amplitudes

[57] The initial sedimentation from bank erosion results in an increased damping of the tidal amplitude (Figure 6b) because of the influence of increased friction on the tidal hydrodynamics. The water level amplitude then increases again over the longer term. This is attributed to the gradual deepening process, which causes the effect of friction to decrease and enhances resonant behavior, as for the FBC. In addition, the widening process results in a geometry that narrows landward and serves to further amplification of the amplitude.

[58] The convergence of estuaries and its impact on the tidal wave characteristics has been subject of extensive earlier research. *Friedrichs and Aubrey* [1994] suggest that convergence of a basin results in an increase in amplitude. On the basis of scaling of the shallow water equations they argue that the advection term (the second term in equation (2)) can be neglected with respect to the other terms for shallow, strongly convergent estuaries. Consequently, the tidal wave energy through a smaller cross section results in an increase of the water level amplitude. *Pillsbury* [1956], *Jay* [1991], *Savenije* [2001], *Savenije and Veling* [2005], and *Prandle* [2003] showed that the water level amplitude can be

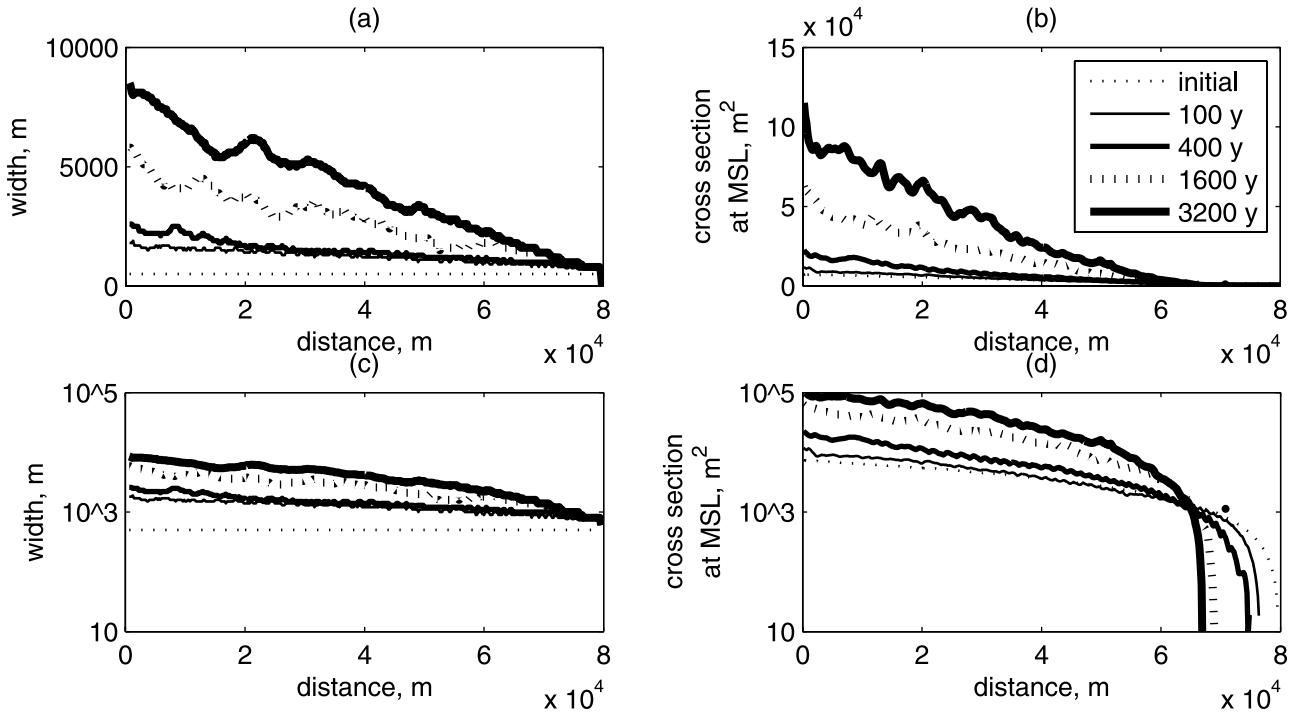

Figure 12. (a) Width development over time along the basin due to bank erosion. (b) Cross-sectional area at MSL over time along the basin. (c) Width development over time along the basin due to bank erosion on a semilog scale. (d) Cross-sectional area at MSL over time along the basin on a semilog scale.

constant along an estuary with an exponentially decaying cross section. The effect of friction, which will decrease the amplitude, is then counterbalanced by the effect of the landward decaying cross section. Typical observation in such an estuary is that the time lag between maximum velocities and maximum water levels is $1/2\pi$ for semi diurnal tidal conditions and that, although the time lag suggests the presence of a standing wave, the tidal wave is progressive in the sense that it still propagates landward. *Pillsbury* [1956] referred to this estuary as an "ideal" estuary, where both the velocity amplitude and the water level amplitude remain constant along the basin. This would lead to constant shear stresses and constant sediment transports.

3.2.3. EBC Velocities, Time Lags, and Ebb/Flow Duration

[59] Model results show indeed that the velocity is relatively constant along the basin for the EBC (Figure 7b) and that the time lags between slack water and MSL (observed after high water) tend toward $1/2\pi$ (Figure 8b). However, Figure 12 shows a linear rather than exponential convergence both in width and cross-sectional area along the basin, although one may argue that the cross-sectional area has a slightly exponential shape, especially in the area midbasin toward the mouth (Figure 12d). We suggest three explanations for this. First, a combination of the linear bank convergence and the reflection of the tidal wave against the head causes the $1/2\pi$ lag in the model results. Research by *Friedrichs and Aubrey* [1994], *Prandle* [2003], and *Savenije and Veling* [2005] do not include reflection of tidal energy against the head as in the current research. Therefore, convergence may remain less than exponential. Second, contrary to an ideal estuary, the tidal amplitude (Figure 6b) increases along the basin, especially on the longer run. This means that, related to a case with constant tidal amplitude along the basin, relatively large cross sections are needed in the landward part to convey the tidal prism. Finally, contrary to assumptions by *Friedrichs and Aubrey* [1994], *Prandle* [2003], and *Savenije and Veling* [2005] the tidal amplitude becomes large compared to the water depth and final amplitude effects cannot be neglected anymore. While it seems likely that this eventual final amplitude effect will have some influence on the final morphology, it is not straightforwardly explained.

[60] It is expected that model runs in a (much) longer basin and in which the tidal wave completely damps because of friction, would show a more pronounced landward exponentially decaying cross section. In that case the $1/2\pi$ time lag between water levels and velocities, which is necessary for zero sediment transport gradients, can only develop because of exponential convergence. Finally, a different formulation of the bank erosion algorithm (especially when it leads to a different characteristic timescale compared to the bed level changes) may result in a different width to depth ratio of the basin.

3.2.4. EBC Relation to Wave Celerity

[61] With respect to the relation between a/h and V_s/V_c, shown in Figure 11b, the embayment maintains larger values for both ratios than in case of the FBC. Also the basin needs more time to adapt to the profile of equation (7). The same observation holds for the time needed to develop toward equal ebb and flood duration, which is shown in Figure 9b.

[62] It can be concluded that, over the longer term, the EBC responds in a similar manner as the FBC, although the large sediment supply from the banks maintains more morphodynamic action after 3200 years than in the case

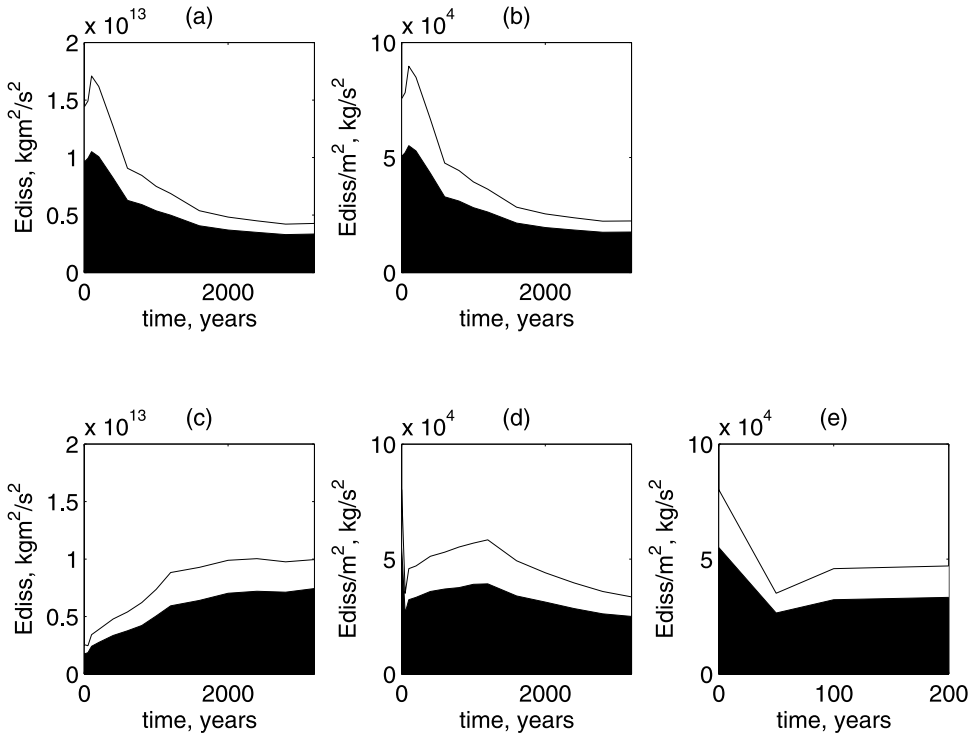

Figure 13. (a) Energy dissipation integrated over the basin area and over one tidal cycle for FBC. (b) Energy dissipation integrated over one tidal cycle per m^2 for FBC. (c) Energy dissipation integrated over the basin area and over one tidal cycle for EBC. (d) Energy dissipation integrated over one tidal cycle per m^2 for EBC. (e) Detail of Figure 13d. The black areas represent the friction parts, and the white areas represent the transport parts.

of the FBC. It is noted that the algorithm for the bank erosion is a rough approximation and does not take explicitly into account the dependency on local values of shear stresses at the bank, sediment/soil characteristics and the exact migration of the banks over time.

3.3. Energy Dissipation

[63] Taking the expression for energy expenditure of *Rodriguez-Iturbe et al.* [1992] as a starting point, the work done by the shear stresses and the transport of sediment in a channel section of length L can be described by the following equation:

$$P = c_f \rho_w \frac{U^2}{R} QL + (\rho_s - \rho_w) gSL, \tag{8}$$

where

P energy dissipation (kg m^2/s^3);
ρ_w water density (kg/m^3);
U velocity (m/s);
R hydraulic radius (m);
Q discharge (m^3/s);
ρ_s sediment density (kg/m^3).

In terms of the current 2-D model parameters and its rectangular grid definition this means that the energy dissipation per grid cell per second at a certain point in time is given by

$$P_{\text{cell}} = \left[g \frac{n^2}{\sqrt[3]{h}} \rho_w \left(\overline{u}^2 + \overline{v}^2\right)^{1.5} + (\rho_s - \rho_w) g \left(S_x^2 + S_y^2\right)^{0.5} \right] dxdy, \tag{9}$$

where

P_{cell} energy dissipation in grid cell (kg m^2/s^3);
$\overline{u}$ depth averaged velocity in x direction (m/s);
$\overline{v}$ depth averaged velocity in y direction (m/s);
S_x, S_y sediment transport in x and y direction (m^3/m/s);
dx, dy length and width of grid cell (m).

In this expression the hydraulic radius (R) was approximated by the water depth (h) under the assumption that the length scale of a grid cell ($\sim$100 m) is much larger than the water depth ($\sim$10 m).

[64] Results are presented in Figures 13 and 14. Figures 13a and 13c show the energy dissipation for the total basin over one tidal cycle for the FBC and EBC, respectively. The part due to friction increasingly dominates the part due to transport in both cases. A closer analysis of the dominant flow parameters in the energy dissipation process follows from a combination of equations (5) and (9), and leads to the following expression:

$$P_{\text{cell}} = \left[\left| \rho_w g n^2 \frac{U^3}{\sqrt[3]{h}} \right| + \left| \frac{0.05}{\Delta D_{50}} \rho_w \sqrt{g} n^3 \frac{U^5}{\sqrt{h}} \right| \right] dxdy. \tag{10}$$

This shows that, for the current model, the friction term (first term on the right hand side) is less influenced by the water depth and the velocity magnitude than the sediment transport term. Lower velocities and larger depths will thus lead to a more dominant impact of friction on the energy dissipation process. Of course this observation strongly depends on formulation of the sediment transport.

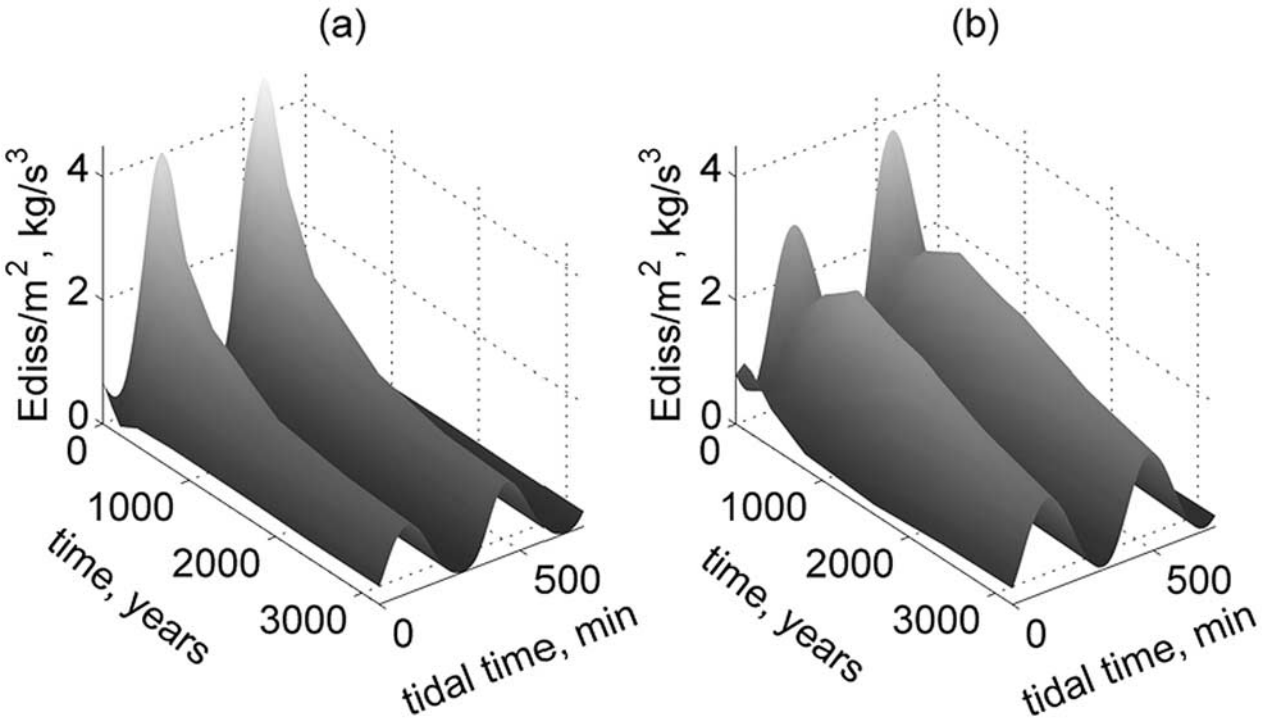

Figure 14. Energy dissipation per m^2 over time (in years) during one tidal cycle (a) for FBC and (b) for EBC. The first peak is related to flood and the second peak to ebb.

[65] The energy dissipation is initially about 5 times larger for the FBC, since the basin is 5 times wider. The energy dissipation of the FBC increases during the first century because of the pattern formation, resulting in increased velocities and the associated larger shear stresses and sediment transports (Figure 7). After one century, the energy dissipation decreases again because of the deeper longitudinal profile and the associated lower velocities. For the EBC, the energy dissipation increases almost continuously because of the widening of the basin, allowing a larger tidal prism to enter the basin (Figure 13c). Figures 13b and 13d show the energy dissipation over one tidal cycle averaged over the basin area at MSL for the FBC and EBC, respectively. Initially they show similar values. The FBC shows the same trend as Figure 13a. However, the dissipation in the EBC drops rapidly within the first 50 years (Figure 13e). This is attributed to the high sedimentation of the basin, which leads to shallow depths and low velocities. After 50 years the averaged energy dissipation increases for the next 1600 years. The trend is largest in the first 100 years due to the pattern formation and then the rate of increase reduces. The continuing increasing trend is attributed to sediment supply due to bank erosion, which leads to a relatively shallow basin with a relatively high impact of the channel-shoal system on the behavior of the flow. The flow is more directed through channels resulting in relatively high velocities and energy dissipation compared to the FBC in which the tide propagates on a more submerged bathymetry. As the profile deepens this effect becomes less pronounced and the energy dissipation decreases for the EBC, in a manner similar to the FBC. Remarkably, the value of the energy dissipation after 3200 years is of the same order of magnitude for both cases.

[66] Figure 14 presents the distribution of energy dissipation over a tidal cycle and shows how this varies over the period modeled (3200 years). Figure 14 shows that initially, for both basins, the energy dissipation during ebb exceeds the dissipation during flood. However, after approximately 3200 years the magnitude of the energy dissipation during ebb and flood is almost similar. Further, there is a shift in timing of the dissipation peaks related to the increasing time lag between maximum water levels and maximum velocities (see Figure 8).

[67] Figure 15 presents results of the tide averaged and flow width averaged energy dissipation along the basin. This shows that the energy dissipation is, in the end, not only decreasing with time, but it is also more uniformly distributed along the basin. The pronounced peaks in the dissipation for the FBC after 3200 years are associated with the presence of bars. This is shown in more detail in Figure 16b, which represents the energy dissipation in the basin in relation to depth contours. The energy dissipation peaks for a morphodynamically relatively stable situation (FBC after 3200 years, Figure 16b) are located at the shoals, whereas more dynamic systems (FBC after 400 years, Figure 16a and EBC after 3200 years, Figure 16c) show major energy dissipation taking place in the channels. This can be explained by the fact that the initial pattern develops on a bathymetry that is on average too shallow. Largest velocities and major transports and shear stresses occur in the channels. As time goes by, the bathymetry deepens and velocities (and the associated shear stresses and transports) decrease. The deepening may continue to such an extent that the shoals remain under water during the tide. Majority of the shear stresses then takes place at the crests of the flooded shoals. As an example, the seaward shoals in

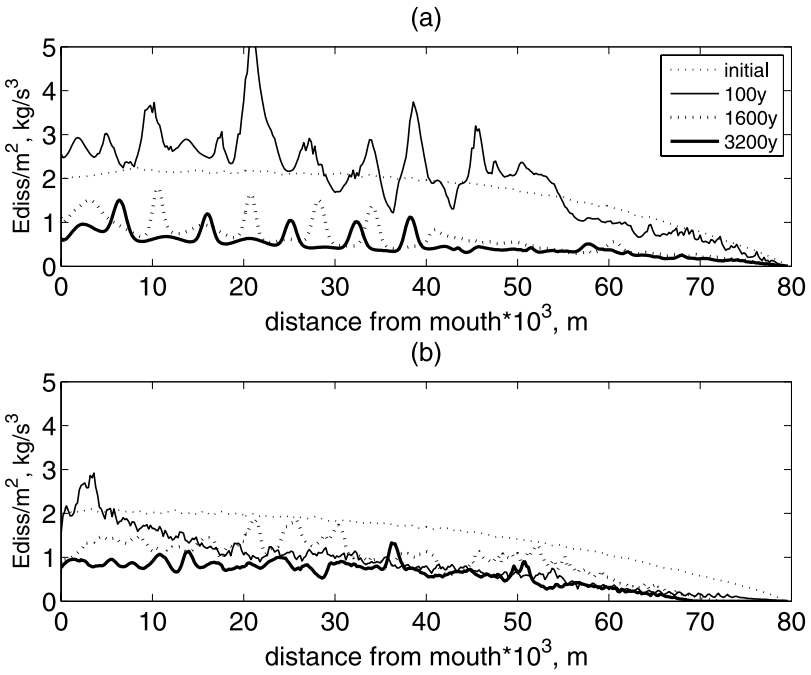

Figure 15. Energy dissipation per m^2 along the basin (kg/s^3) averaged over one tidal cycle and the flow width (a) for FBC and (b) for EBC.

Figure 16b are completely drowned (with energy dissipation peaks at the crest), whereas toward the head the shoals are present as intertidal area (with energy dissipation peaks in the channels).

[68] It can be argued that the energy dissipation peaks at the shoals are a consequence of the confinement of the FBC, because it forces the flow to "bounce" over the shoals. The EBC would not lead to such a system since, during its morphological evolution, the major flow would continuously use channels. This is reflected for the EBC in Figure 15b showing no pronounced peaks to the extent present in the FBC (Figure 15a).

4. Validation

[69] Data on morphological evolution in estuaries and the assumed decreasing energy dissipation over relatively long time spans (~centuries) are not readily available, because detailed measurements have only been carried out during the last decades or century. Furthermore, where relatively long-term data are available, human intervention (i.e., by access channel dredging, the construction of flow mitigating structures or land reclamation) has invariably had a high impact on the estuarine bathymetry. Finally, sea level rise would also be of importance on a timescale of centuries.

[70] When values of energy dissipation are derived using a 2-D numerical model for a specific estuary, on the basis of different historical bathymetries, this leaves the question open as to whether this should be attributed to the system, human intervention or sea level rise. For example, research by *Lane* [2004] and *Blott et al.* [2006] shows major changes of the Mersey estuary bathymetry (UK) over the last century, which is attributed to training wall construction and dredging. Their research was based on analysis of historical bathymetric charts and runs of a numerical flow model. However, no distinction could be made between the subsequent effects of sea level rise and eventual wave climate changes or autonomous evolution (the latter is not mentioned in their research).

[71] Validation may take place in terms of the order of magnitude of the actual energy dissipation for a numerical model based on a real geometry and bathymetry. *Winterwerp et al.* [2001] show an application of such a model considering

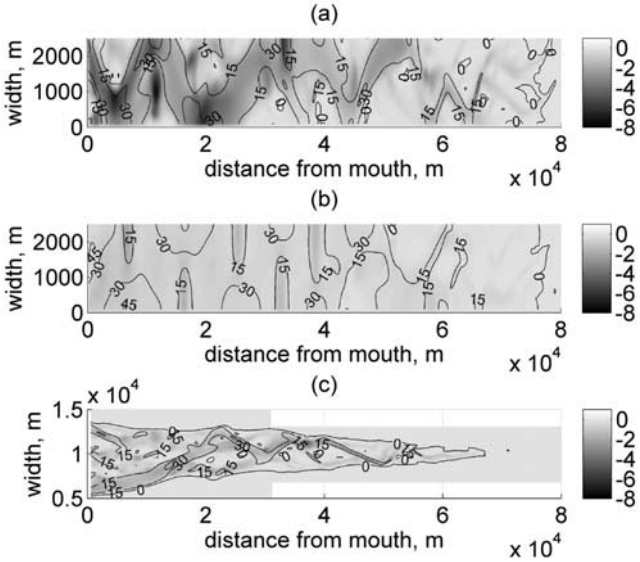

Figure 16. Energy dissipation per m^2 (kg/s^3) averaged over one tidal cycle and depth contour lines with respect to MSL (a) for FBC at 400 years, (b) for FBC at 3200 years, and (c) for EBC at 3200 years.. Negative values indicate higher dissipation.

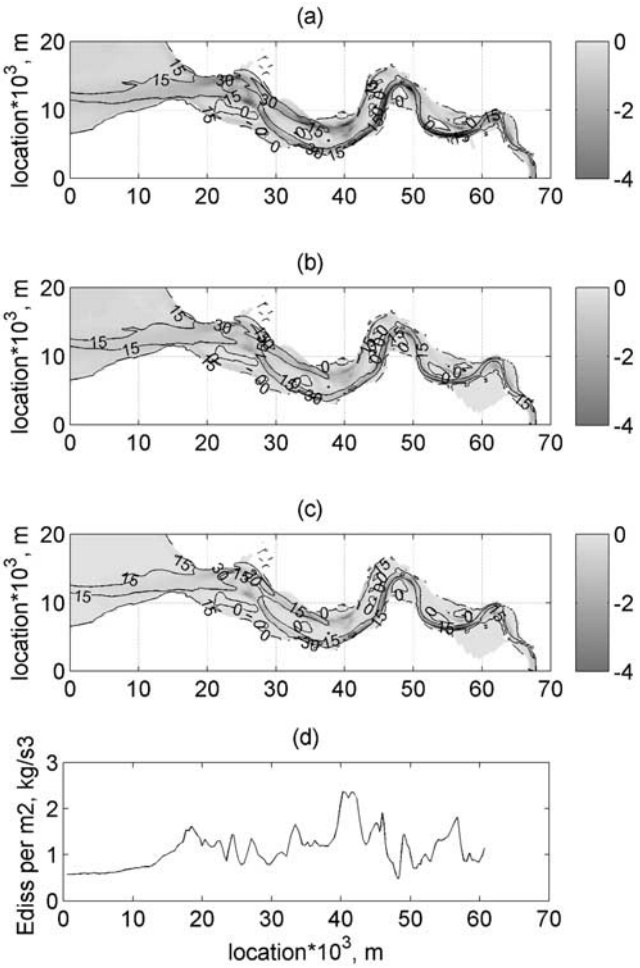

Figure 17. Western Scheldt energy dissipation per m^2 (kg/s^3) averaged over one tidal cycle and depth contour lines with respect to MSL (a) for total energy dissipation, (b) for contribution of friction, (c) for contribution of sediment transport, and (d) for energy dissipation per m^2 along the basin (kg/s^3) averaged over one tidal cycle and the width. More negative values indicate higher dissipation. Cross sections were taken perpendicular to the main flow direction.

the Western Scheldt, whereas *Kuijper et al.* [2004] give details on the validation of a similar Western Scheldt model, in which geometry, grid cell sizes, time steps and forcing were similar to the current model. Figure 17 shows an overview of the results of this model on the basis of a 1998 bathymetry and applying astronomic boundary conditions.

[72] The Western Scheldt itself is a relatively young estuary that developed early in the Middle Ages when a tidal channel penetrated landward toward the Scheldt River, located north of Antwerp, where it initially developed over a bed of marshland [*van der Spek*, 1997; *Beets and van der Spek*, 2000]. Alluvial sand and remnants of erosion resistant peat layers determine the present bathymetry. Land reclamation taking place over several centuries resulted in dikes constructed on the banks of the Western Scheldt, including scour protection at the bed sometimes extending into the deepest channels adjacent to the dikes.

[73] Figure 17 shows that the order of magnitude of energy dissipation is similar to the model results. The peak dissipation found in the relatively narrow section at km 40 from the mouth and the smaller peaks along the basin are attributed to narrowing by land reclamation works and nonerodible peat layers. This can be considered as a physical constraint of the system, preventing it from evolving toward a most probable state with a more gradual and uniform distribution of energy dissipation, which will be subject of discussion in the next section.

[74] Figure 17 shows only part of the Western Scheldt which in reality extends more landward and narrows extensively into the Scheldt River. This is outside the domain of the current model, which focuses on the relatively broad and tide dominated area of the Western Scheldt. The presence of the river Scheldt may explain the relatively constant energy dissipation value still present at 60 km from the mouth, contrary to the zero energy dissipation of the current model, and suggests that still considerable tidal energy is present in this section. This is confirmed by *van der Spek* [1997] and *Kuijper et al.* [2004] who describe large landward amplifications of the tidal amplitude that only damp beyond Antwerp.

5. Discussion

5.1. Grid Resolution

[75] The results presented thus far, assume that the channel shoal pattern may be described by grid cell sizes of 100 by 200 m. This puts a limit to the minimum spatial scale the model is able to resolve. On the seaward side of the embayment this may be acceptable, since in that area large tidal prisms generate relatively large spatial patterns. For the cross section, for example, this is confirmed by empirical relationships between tidal prism and cross-sectional area suggested by *Jarrett* [1976]. Further, *van der Wegen and Roelvink* [2008] suggest a relationship between a characteristic longitudinal morphological length scale and the tidal prism on the basis of their model results. Also the characteristic morphological length scales are much larger than the applied grid size. More landward, however, the tidal prism and channel cross section become smaller and grid resolution starts to have a larger impact on an accurate description of the channel cross section, up to the extent that the grid cannot describe the channels anymore.

[76] An additional model run was carried out with a grid size of 33 m by 67 m, which is three times smaller than in the original model. Because of the long calculation duration involved (~4 weeks), this was done for a relatively short, 20 km long, basin for 600 years with similar model settings as the current model (see for a closer description of the short basin model with coarse grid *van der Wegen et al.* [2007]). The geometry of this model resembles the landward final 20 km of the current model, in the sense that it has equal basin size and that the bed levels and percentage of intertidal area are similar.

[77] Comparison of Figures 18a and 18b shows that major pattern characteristics are maintained for the finer grid, especially near the mouth, where one distinguishes a single main channel with similar size. Compared to the coarse grid model, the fine grid model shows more detail especially near the head (i.e., shoals within the main

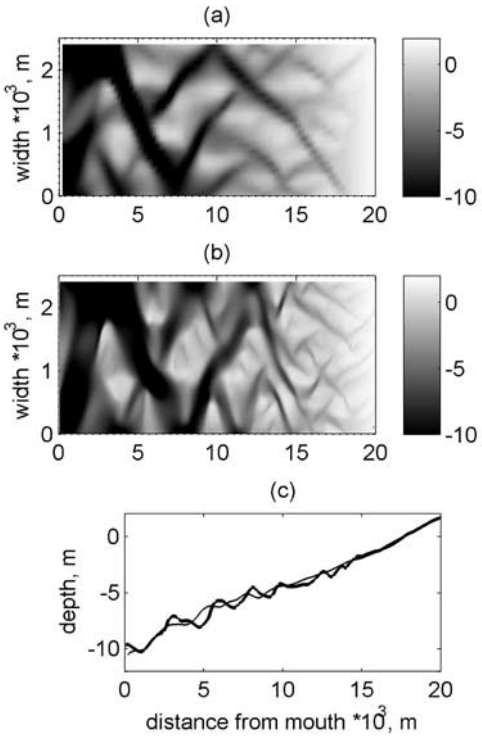

Figure 18. Bed levels after 600 years for 2.5 km wide and 20 km long basin (a) with coarse grid 100 × 200 m, (b) with fine grid 33 × 67 m, and (c) width-averaged longitudinal bed profile for coarse grid (thin line) and fine grid (thick line).

channel, more channel curvature and the presence of smaller channels) and the difference with the coarse grid model in that area is relatively large. The comparison suggests that seaward the impact of grid size reduces and that small-scale patterns do not impact on the major morphodynamic features. No distinct differences were observed in the width averaged longitudinal bed profiles (Figure 18c). For the current 80 km long basin, this suggests that the coarse grid qualitatively resolves major pattern characteristics for a large part of the long basin.

5.2. Sea Level Rise

[78] *Fleming et al.* [1998] conclude that, after a period of rapid sea level rise, sea level has been relatively constant over the past 6000 years, although still uncertainty exists on the extent of fluctuations during this period. On the basis of observations, *Dronkers* [1986], *Woodroffe et al.* [1993], *Pethick* [1994], *Rees et al.* [2000], and *Beets and van der Spek* [2000] suggest that the relatively constant sea level created conditions for considerable infill of different basins and river valleys that were previously drowned by the rapid sea level rise.

[79] Sea level rise is absent in the current model setup. In this way, development of equilibrium could be investigated under constant boundary conditions. The current research suggests that major morphodynamic adaptations of alluvial coastal plain estuaries are covered within the timeframe of the recent relatively constant sea level (∼millennia), provided that there is enough sediment available. Concerning the small life span of about 800 years of the Western Scheldt estuary and the fact that it developed over shallow, drowned marshland, model results would imply that the estuary is yet far from equilibrium. However, for a more thorough analysis a number of additional processes should be taken into account, like, for example, bed composition, the existence of nonerodible layers, wave driven transport at the mouth and the bathymetry seaward from the mouth. Furthermore, this research leaves the question how coastal plain estuaries would respond to the relatively small fluctuations in sea level rise over the past 6000 years suggested by *Fleming et al.* [1998]. These small fluctuations in sea level, not only affecting MSL but also the character of the tide at the mouth, could have a considerable impact. This will be subject of future research.

5.3. Initial Conditions

[80] Contrary to the observed basin infill due to sea level rise mentioned in the last section, the current model shows a continuous sediment export. One explanation for this might be the modeling approach not taking into account finer sediments and settling lag effects. Another possible explanation is that the initial condition was taken too shallow in order to stimulate pattern formation and to relate it to the current Western Scheldt bathymetry.

[81] A number of reasons may be responsible for the shallowness of the Western Scheldt estuary. First, it developed only about 800 years ago, which means that it was not drowned to the extent of river valleys during the period of rapid sea level rise and that the period for pronounced further deepening has been too short. Second, the presence of nonerodible layers may have prevented the Western Scheldt basin from deepening further. However, *Dronkers* [1998] considers these reasons not being dominant suggesting that the estuary is close to equilibrium. He attributes this is to a strong M4 component being present outside the mouth on the relatively shallow continental shelf. The current model only prescribes a sine shaped seimidiurnal water level at the seaward boundary and would therefore not lead to importing conditions. Further, wave induced transport from adjacent coastlines and the ebb tidal delta, the occurrence of storm events and sea level rise might play an important role as well.

[82] It is questioned whether another, for example deeper or more gently sloped, initial condition would lead to similar results. Sensitivity analysis in this respect was not carried out, because of the long computation time involved (∼months). Another problem would be the long adaptation timescale that may finally lead to a similar result, but not within the timeframe considered (∼4000 years). This would especially hold for configurations with deeper initial conditions which will transport less sediment. It is believed that similar results will be obtained in terms of characteristic morphological length scales, especially in relation to local flow conditions. The width averaged longitudinal profile could be subject to (apart from the local disturbances by shoals) a horizontal shift landward when the initial profile is relatively deep and seaward for shallower initial conditions (for a 1-D configuration this is confirmed by *van der Wegen and Roelvink* [2008]). The seaward shift will be caused by rapid sedimentation at the head. Since the impact of friction for such a shallow basin remains relatively high, the tidal

amplitude may remain damped and no resonant tidal behavior may occur.

[83] Another important initial condition is that the banks were set at a level higher than the expected highest water level in the basin. This was done since preliminary calculations showed considerable infill of the basin when banks were flooded at a certain moment because of the resonant tidal wave. This delayed the evolution considerably and complicated the analysis of the results. Furthermore, lower bank levels (below high water or even below MSL) would lead to large and extending amount of intertidal area and a system quite different than the reference case of the Western Scheldt estuary. *Marciano et al.* [2005] describe an example of the evolution of such a basin, i.e., a typical inlet in the Dutch Waddenzee area, following a similar process-based approach. A more extended intertidal area would probably influence final basin characteristics by means of different intertidal flat flooding and draining characteristics (described, for example, in more detail by *D'Alpaos et al.* [2005] for the Venice lagoon), and its impact on tidal wave propagation and dominant sedimentation processes. These may include for example settling lags and erosion lags and the impact of vegetation as described by *D'Alpaos et al.* [2007] and *Murray et al.* [2007]. Whether or not such a system would finally lead to decreasing basin wide energy dissipation needs to be confirmed by future research.

[84] Considering further the impact of initial conditions on energy dissipation, for optimal fluvial networks, *Rinaldo et al.* [2006] suggest that initial (and boundary) conditions affect the feasible optimal state of the network. This means that initial conditions influence the final values of minimum energy dissipation so that different initial conditions could possibly lead to a more optimal network state as well as lower values for the energy dissipation. This may also hold for this tidal configuration especially considering the assumed shift of the longitudinal profile. Closer analysis is considered to be outside the scope of the current research.

5.4. Energy Dissipation

[85] The major processes taking place in the basins (short-term pattern formation and long-term deepening and widening) are well reflected by the evolution of the energy dissipation. Also, the lower state of morphodynamic activity, especially apparent in the FBC for the period considered, agrees well with the decreasing (rate of) energy dissipation.

[86] *Rodriguez-Iturbe et al.* [1992] use their energy dissipation formulation to show that their considered drainage network develops toward a state of minimum energy dissipation. The current model leads to a similar conclusion. However, *Rodriguez-Iturbe et al.* [1992] consider a loopless network with fixed links between flow sections, whereas the current research describes a dynamic evolution, that allows for slowly migrating bars and channel configurations, local peaks in energy dissipation shifting along the basin, flow across tidal flats, and even loops developing in the channel network. Therefore, it is difficult to compare the current model results to their first two underlying principles (i.e., the principle of minimum energy dissipation in any link of the network, and the principle of equal energy dissipation per unit channel anywhere in the network), although their third and final principle of minimization of energy dissipation in the network as a whole seems to be confirmed by the current research considering the current model domain as the "network."

[87] More pronounced and in apparent contradiction to these three principles are the effects of pattern formation and bank erosion, since both processes lead to a temporal increase in the overall basin energy dissipation. This is attributed to the initial condition prescribing a flat bed, which imposes an inherent instability to the system that the processes seek to adjust. During a representative adaptation period, in which the dominant patterns develop, the geometry is formed that fulfills the conditions of the system. After the adaptation period the energy dissipation decreases at a decreasingly lower rate and even becomes less than at the initial, flat state.

5.5. Energy Flux

[88] These findings can be linked to equilibrium conditions derived from an entropy based approach in research by *Leopold and Langbein* [1962], *Townend* [1999], *Townend and Dun* [2000]. The latter two references are more specifically related to estuarine environments and use the criterion of constant entropy production rate per unit discharge to suggest that the longitudinal energy flux distribution along an estuary can be described by an exponentially decreasing function. Their reasoning is briefly repeated here for reasons of clarity.

[89] *Leopold and Langbein* [1962] introduce the principle that river systems aim for least work, which may be interpreted as minimum production of entropy. They suggest that this state will be reached when the rate of entropy production per unit discharge is constant along a river and is proportional to the longitudinal gradient of energy dissipation, which is expressed in the following relation:

$$\frac{1}{Q}\frac{d\varphi}{dt} = \frac{1}{H}\frac{dH}{dx} = a, \tag{11}$$

where

$d\varphi$ entropy production (m^2);
dt time span (s);
dH loss of energy head over distance dx (m);
Q discharge (m^3/s);
H energy head relative to some datum (m);
a constant (m^{-1}).

Langbein [1963] applied this theory to estuaries as well, albeit for a highly schematized case in which the amplitudes of the water level and the velocity are assumed constant along the estuary and in which friction and overtides are disregarded.

[90] Considering that estuaries, contrary to river systems, are governed by time and directionally varying discharges over the tide, *Townend* [1999] suggests that the rate of entropy production per unit discharge for estuaries can be expressed by evaluating the energy flux instead of the energy head. He thus proposed

$$\frac{1}{Q}\frac{d\varphi}{dt} = \frac{1}{HQ}\frac{d(HQ)}{dx}. \tag{12}$$

Further, *Townend* [1999] follows the suggestion by *Leopold and Langbein* [1962] that the most probable state of the

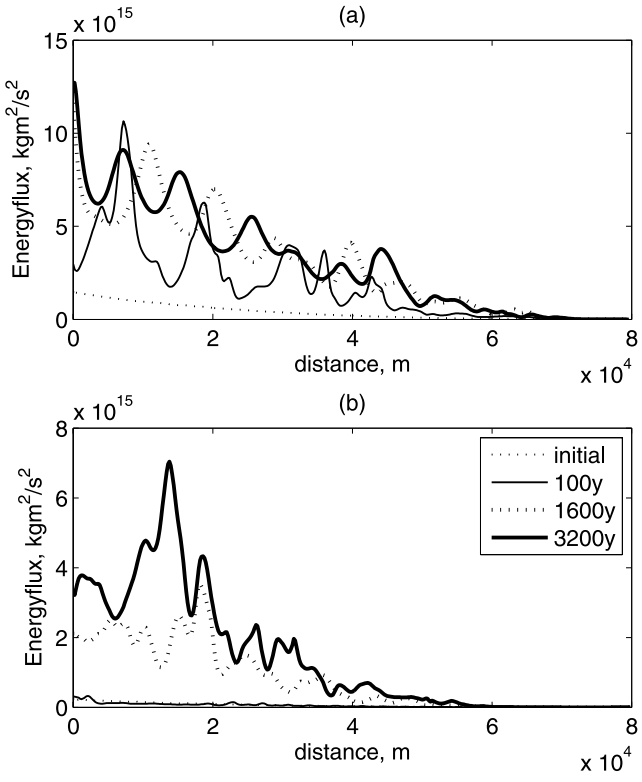

Figure 19. Width-integrated energy flux distribution along the basin (a) for FBC and (b) for EBC.

estuarine geometry would be reached when the rate of entropy production is constant. This yields

$$\frac{1}{HQ}\frac{d(HQ)}{dx} = a. \tag{13}$$

Solving equation (13) and considering integration over a complete tidal period (T) yields with (α) and (β) being constants

$$\rho g \int_0^T HQdt = \exp(\alpha x + \beta). \tag{14}$$

Equation (14) suggests that for a constant production of entropy per unit discharge the energy transported because of the tidal wave will decay exponentially landward. *Townend and Dun* [2000] showed that the equation leads to good results for the Humber estuary and the Bristol Channel in the UK. In case of the Humber small discrepancies between equation (14) and 1-D model results were attributed to the effect of river discharge and the effect of the construction of training work. Even evolution toward a better fit to equation (14) was suggested by using different historical bathymetries ranging over 150 years. For the Bristol Channel deviations between equation (14) and a 2-D model were attributed to the geology of the basin having only limited sediment supply and hard banks, both opposing further evolution toward the most probable state. Comparison to a third estuary, Southampton Water, showed less favorable results. 1-D model results showed a linear relationship between distance from the mouth and energy flux. This was attributed to the rather rectangular geometry of the basin with only little supply of sediments for further evolution.

[91] Figure 19 shows the evolution of the current model in terms of the left side of equation (14) taking absolute values for (HQ). Apart from the anomalies caused by the channel-shoal pattern, the FBC continuously shows a linear relationship between distance from the mouth and energy flux just like in case of Southampton Water. The linear relationship suggests uniform work or constant energy dissipation along the basin, contrary to equation (13)

$$\frac{d(HQ)}{dx} = \text{constant}. \tag{15}$$

Occurrence of uniform energy dissipation is supported by Figure 15a.

[92] Compared to the FBC, the EBC shows a more exponential relationship similar to equation (14), although it only becomes apparent on the longer term and, still, longitudinal deviations are large because of the channel-shoal pattern. Also, the exponential distribution is not outspoken and may even be questionable. A linear distribution is more supported by the fact that, like in the fixed basin configuration, longitudinal energy dissipation is rather uniform along the basin (see Figure 16b) and by the fact that the basin shows a linear rather than an exponential widening of the banks toward the mouth, see Figure 12.

[93] The fact that both configurations aim for uniform distribution of energy dissipation along the basin, contrary to uniform work described by equation (13), suggests that the most probable state of the system described by the hydrodynamic and morphodynamic equations (1)–(5) is not reached. Assuming the validity of equation (13), a first possible explanation could be that the linear decrease of energy head observed along the estuary does not necessarily contradict equation (13). This holds, for example, for the case when the discharge integrated over the tide decreases exponentially along the basin, whereas the energy head still decreases linearly. Equation (13) is then dominated by the along basin discharge profile.

[94] A second possible explanation is the occurrence of inherent constraints in the definition of the model configurations. Apart from the definition of fixed banks, the prescribed length of the basin can be considered a constraint as well. On the longer run, resonance develops in the basin leading to larger water level amplitudes, especially near the head. For the EBC, the defined bank level at MSL + 3.2 m prevents the areas near the head from flooding. In case that the basin would not have been blocked at the head and that bank level would have been lower, flooding would occur at the head because of the landward increasing tidal amplitude. This would possibly result in a longer basin with a landward exponentially converging width. Such a basin could lead to better agreement with equations (13) and (14). The tidal dynamics of such a long, strongly converging type of estuary have been extensively studied (among others by *Jay* [1991], *Friedrichs and Aubrey* [1996], *Prandle* [2003], *Savenije and Veling* [2005], and *Toffolon et al.* [2006]) although none of the studies were carried out on the basis of an explicit morphodynamic formulation like in the current process-based approach.

[95] The Western Scheldt estuary has weakly converging width [*Savenije and Veling*, 2005; *Toffolon and Crosato*, 2007]. Despite the fact that the size of the current model configuration was inspired by this estuary, the model does not reproduce such geometry. Assuming that the current models' bank erosion algorithm is adequate enough, probable reasons for this are the facts that the Western Scheldt is relatively young, its banks are protected by dikes and that its 70 km long narrow river section is not taken into account in the current model.

6. Conclusions

[96] The long-term, process-based approach of the current research shows evolution of morphodynamic features and timescales that are comparable to estuarine morphodynamics found in reality. This is despite a relatively simple system of shallow water equations and a straightforward formulation of the sediment transport. A major shortcoming is the computational time required (∼weeks for 3200 years), so that relatively few runs have been carried out for the current research.

[97] The basins under consideration evolve toward a state of less morphodynamic activity, represented by relatively stable characteristic patterns and decreasing deepening and widening of the basins. This is despite observations that there remains a continuous sediment export toward the sea and that bar and shoal migration continues to take place. Closer analysis of the hydrodynamic characteristics over time shows lower width averaged velocity amplitudes, similar ebb and flood duration and velocities along the basin, constant time lags between maximum velocities and maximum water levels and a stable (a/h) and (V_s/V_c) relationship. With respect to the latter, it is suggested that equilibrium conditions are formed by two balancing effects on the tidal wave celerity, namely the effect of storage and the effect of tidally fluctuating water levels. The effect of friction on the tidal asymmetry, implicitly also present in the factor (a/h), can apparently be neglected. A probable explanation is that after 3200 years both basins reflect a situation in which a standing wave is present. In that case, ebb and flood velocities take place at equal water levels and their magnitude becomes similar, so that the effect of friction is equal during ebb and flood and it has no effect anymore on tidal asymmetry.

[98] The current research shows that energy dissipation reflects the major processes and their timescales (pattern formation, widening and deepening). Pattern formation and bank erosion both cause an initial and temporal increase in energy dissipation. On the longer term, however, the basin wide energy dissipation decreases at decreasingly lower rate and becomes more uniformly distributed along the basin.

[99] Comparison of the model results to a 2-D numerical model describing a comparable basin (Western Scheldt) shows that the order of magnitude of the energy dissipation and its relatively uniform width-averaged longitudinal distribution are indeed similar. Deviations are attributed to bank protection works and the small current model domain that excludes the narrow landward section of the Western Scheldt and in which the tidal wave propagates.

[100] Comparison of the model results to equilibrium conditions defined by minimum entropy production, or, constant entropy production rate, suggests that the fixed banks and the prescribed level of the banks in combination with the prescribed length of the estuary prevent the chosen hydrodynamic and morphodynamic model formulations from evolving toward the most probable state.

[101] **Acknowledgments.** In the preparation and literature review for this work use was made by two reports that both extensively review the state of the art of current research and knowledge on estuarine morphodynamics. These are reports by WL Delft Hydraulics *Wang et al.* [1999] and *Department for Environment*, Food and Rural Affairs/Environment Agency [2005]. Both reports made the preparations of the current work much more efficient and enjoyable. The extensive comments of associate editor Brad Murray, reviewer Ian Townend, and two other anonymous reviewers were highly appreciated and contributed substantially to the quality of the work. Further, the authors are grateful to the UNESCO-IHE research fund for making this research financially possible.

References

Ahnert, F. (1960), Estuarine meanders in the Chesapeake Bay area, *Geogr. Rev.*, *50*, 390–401, doi:10.2307/212282.

Airy, G. B. (1845), Tides and waves, in *Encyclopedia Metropolitana*, vol. 5, edited by E. Smedley and H. J. Rose, pp. 241–396, B. Fellows, London.

ASCE Task Committee on Hydraulics, Bank Mechanics, and Modeling of River Width Adjustment (1998a), River width adjustment. part I: Processes and mechanisms, *J. Hydraul. Eng.*, *124*(9), 881–902, doi:10.1061/(ASCE)0733-9429(1998)124:9(881).

ASCE Task Committee on Hydraulics, Bank Mechanics, and Modeling of River Width Adjustment (1998b), River width adjustment. part II: Modeling, *J. Hydraul. Eng.*, *124*(9), 903–917, doi:10.1061/(ASCE)0733-9429(1998)124:9(903).

Bagnold, R. A. (1966), An approach to the sediment transport problem, *U.S. Geol. Surv. Prof. Pap. 422-I*, U.S. Geol. Surv., Reston, Va.

Beets, D. J., and A. J. F. van der Spek (2000), The holocene evolution of the barrier and the back-barrier basins of Belgium and the Netherlands as a function of late Weichselian morphology, relative sea-level rise and sediment supply, *Neth. J. Geosci.*, *79*(1), 3–16.

Blott, S. J., K. Pye, D. Van der Wal, and A. Neal (2006), Long-term morphological change and its causes in the Mersey Estuary, NW England, *Geomorphology*, *81*, 185–206, doi:10.1016/j.geomorph.2006.04.008.

Boon, J. D., III, and R. J. Byrne (1981), On basin hypsometry and the morphodynamic response of coastal inlet systems, *Mar. Geol.*, *40*, 27–48, doi:10.1016/0025-3227(81)90041-4.

D'Alpaos, A., S. Lanzoni, and M. Marani (2005), Tidal network ontogeny: Channel initiation and early development, *J. Geophys. Res.*, *110*, F02001, doi:10.1029/2004JF000182.

D'Alpaos, A., S. Lanzoni, M. Marani, and A. Rinaldo (2007), Landscape evolution in tidal embayments: Modeling the interplay of erosion, sedimentation, and vegetation dynamics, *J. Geophys. Res.*, *112*, F01008, doi:10.1029/2006JF000537.

Department for Environment, Food and Rural Affairs/Environment Agency (2005), Review and formalisation of geomorphological concepts and approaches for estuaries, *Rep. FD2116/TR2*, Lincoln, United Kingdom.

De Vriend, H. J. (1996), Mathematical modelling of meso-tidal barrier island coasts. part I: Emperical and semi-emperical models, in *Advances in Coastal and Ocean Engineering*, edited by P. L. F. Liu, pp. 115–149, World Sci., Hackensack, N. J.

Dronkers, J. (1986), Tidal asymmetry and estuarine morphology, *Neth. J. Sea Res.*, *20*, 117–131, doi:10.1016/0077-7579(86)90036-0.

Dronkers, J. (1998), Morphodynamics of the Dutch Delta, in *Physics of Estuaries and Coastal Seas*, edited by J. Dronkers and M. B. A. M. Scheffers, pp. 297–304, Balkema, Rotterdam, Netherlands.

Engelund, F. and E. Hansen (1967), *A Monograph on Sediment Transport in Alluvial Streams*, Teknisk Forlag, Copenhagen.

Feola, A., E. Belluco, A. D'Alpaos, S. Lanzoni, M. Marani, and A. Rinaldo (2005), A geomorphic study of lagoonal landforms, *Water Resour. Res.*, *41*, W06019, doi:10.1029/2004WR003811.

Fleming, K., P. Johnston, D. Zwartz, Y. Yokoyama, K. Lambeck, and J. Chappell (1998), Refining the eustatic sea-level curve since the Last Glacial Maximum using far- and intermediate-field sites, *Earth Planet. Sci. Lett.*, *163*(1–4), 327–342, doi:10.1016/S0012-821X(98)00198-8.

Friedrichs, C. T., and D. G. Aubrey (1988), Non-linear tidal distortion in shallow well mixed estuaries: A synthesis, *Estuarine Coastal Shelf Sci.*, *27*, 521–545, doi:10.1016/0272-7714(88)90082-0.

Friedrichs, C. T., and D. G. Aubrey (1994), Tidal propagation in strongly convergent channels, *J. Geophys. Res.*, *99*(C2), 3321–3336, doi:10.1029/93JC03219.

Friedrichs, C. T. and D. G. Aubrey (1996), Uniform bottom shear stress and equilibrium hypsometry of intertidal flats, in *Mixing in Estuaries and Coastal Seas*, edited by C. Pattiaratchi, pp. 405–429, AGU, Washington, D.C.

Friedrichs, C. T., D. G. Aubrey, and P. E. Speer (1990), Impacts of relative sea-level rise on evolution of shallow estuaries, in *Coastal and Estuarine Studies*, vol. 38, *Residual Currents and Long-Term Transport*, edited by R. T. Cheng, pp. 105–122, Springer-Verlag, New York.

Groen, P. (1967), On the residual transport of suspended matter by an alternating tidal current, *Neth. J. Sea Res.*, *3*(4), 564–574, doi:10.1016/0077-7579(67)90004-X.

Hayes, M. O. (1975), Morphology of sand accumulation in estuaries: An introduction to the symposium, in *Estuarine Research II*, edited by L. E. Cronin, pp. 3–22, Academic, San Diego, Calif.

Hibma, A., H. J. de Vriend, and M. J. F. Stive (2003a), Numerical modeling of shoal pattern formation in well-mixed elongated estuaries, *Estuarine Coastal Shelf Sci.*, *57*(5–6), 981–991, doi:10.1016/S0272-7714(03)00004-0.

Hibma, A., H. M. Schuttelaars, and H. J. de Vriend (2003b), Initial formation and long-term evolution of channel-shoal patterns in estuaries, in *Proceedings of the Third* International Association of Hydraulic Engineering and Research *Symposium on River, Coastal and Estuarine Morphodynamics*, edited by A. Sánchez -Acrilla and A. Bateman, pp. 740–760, Int. Assoc. of Hydraul. Eng. and Res., Barcelona, Spain.

Horton, R. E. (1945), Erosional development of streams and their drainage basins: Hydrophysical approach to quantitative morphology, *Geol. Soc. Am. Bull.*, *56*, 275–370, doi:10.1130/0016-7606(1945)56[275:EDOSAT]2.0.CO;2.

Ikeda, S. (1982), Lateral bed load transport on side slopes, *J. Hydraul. Div. Am. Soc. Civ. Eng.*, *108*(11), 1369–1373.

Ikeda, S., and T. Aseada (1983), Sediment suspension with rippled bed, *J. Hydraul. Eng.*, *109*(3), 409–423.

Jarrett, J. T. (1976), Tidal prism-inlet relationships, *Gen. Invest. Tidal Inlets Rep. 3*, 32 pp., U.S. Army Coastal Eng. and Res. Cent., Fort Belvoir, Va.

Jay, D. A. (1991), Green's law revisited: Tidal long wave propagation in channels with strong topography, *J. Geophys. Res.*, *96*(C11), 20,585–20,598, doi:10.1029/91JC01633.

Kirchner, J. W. (1993), Statistical inevitability of Horton's laws and the apparent randomness of stream channel networks, *Geology*, *21*, 591–594.

Kuijper, C., R. Steijn, D. Roelvink, T. van der Kaaij, and P. Olijslagers (2004), Morphological modelling of the Western Scheldt: Validation of Delft3D, *WL Delft Hydraul. Rep. Z3648*, WL Delft Hydraul., Delft, Netherlands.

Lane, A. (2004), Bathymetric evolution of the Mersey Estuary, UK, 1906–1997: Causes and effects, *Estuarine Coastal Shelf Sci.*, *59*, 249–263, doi:10.1016/j.ecss.2003.09.003.

Langbein, W. B. (1963), The hydraulic geometry of a shallow estuary, *Bull. Int. Assoc. Sci. Hydrol.*, *8*, 84–94.

Lanzoni, S., and G. Seminara (2002), Long-term evolution and morphodynamic equilibrium of tidal channels, *J. Geophys. Res.*, *107*(C1), 3001, doi:10.1029/2000JC000468.

Latteux, B. (1995), Techniques for long-term morphological simulation under tidal action, *Mar. Geol.*, *126*, 129–141, doi:10.1016/0025-3227(95)00069-B.

Leendertse, J. J. (1987), A Three-Dimensional Alternating Direction Implicit Model With Iterative Fourth Order Dissipative Non-Linear Advection Terms, *WD-3333-NETH*, Rijkswaterstaat, Utrecht, Netherlands.

Leopold, L. B. and W. B. Langbein (1962), The concept of entropy in landscape evolution, *U.S. Geol. Surv. Prof. Pap. 500-A*, pp. A1–A20, U.S. Geol. Surv., Reston, Va.

Lesser, G. R., J. A. Roelvink, J. A. T. M. Van Kester, and G. S. Stelling (2004), Development and validation of a three-dimensional morphological model, *Coastal Eng.*, *51*, 883–915, doi:10.1016/j.coastaleng.2004.07.014.

Marciano, R., Z. B. Wang, A. Hibma, H. J. de Vriend, and A. Defina (2005), Modelling of channel patterns in short tidal basins, *J. Geophys. Res.*, *110*, F01001, doi:10.1029/2003JF000092.

Murray, A. B., M. A. F. Knaappen, M. Tal, and M. L. Kirwan (2007), Biomorphodynamics in river, coastal and estuarine settings, paper presented at 5th International Association of Hydraulic Engineering and Research Conference on River, Coastal and Estuarine Morphodynamics, Int. Assoc. of Hydraul. Eng. and Res., Enschede, Netherlands.

Parker, B. B. (Ed.) (1991), *Tidal Hydrodynamics*, John Wiley, New York.

Pethick, J. S. (1994), Estuaries and wetlands: Function and form, in *Wetland Management*, edited by R. A. Falconer and P. Goodwin, pp. 75–87, Thomas Telford, London.

Pillsbury, G. (1956), *Tidal Hydraulics*, Corps Eng., Vicksburg, Miss.

Prandle, D. (2003), Relationship between tidal dynamics and bathymetry in strongly convergent estuaries, *J. Phys. Oceanogr.*, *33*, 2738–2750, doi:10.1175/1520-0485(2003)033<2738:RBTDAB>2.0.CO;2.

Prandle, D. (2004), Sediment trapping, turbidity maxima, and bathymetric stability in macrotidal estuaries, *J. Geophys. Res.*, *109*, C08001, doi:10.1029/2004JC002271.

Pritchard, D. W. (1952), Estuarine hydrography, in *Advances in Geophysics*, vol. 1, edited by H. E. Landsberg, pp. 243–245, Academic, New York.

Pritchard, D. (2005), Suspended sediment transport along an idealized tidal embayment: Settling lag, residual transport and the interpretation of tidal signals, *Ocean Dyn.*, *55*, 124–136, doi:10.1007/s10236-005-0004-7.

Rees, J. G., J. Ridgway, S. Ellis, R. W. O. Knox, R. Newsham, and A. Parkes (2000), Holocene sediment storage in the Humber Estuary, in *Holocene Land-Ocean Interaction and Environmental Change Around the North Sea*, edited by I. Shennan and J. E. Andrews, pp. 119–143, Geol. Soc., London.

Reynolds, O. (1887), On certain laws relating to the régime of rivers and estuaries and on the possibility of experiments on a small scale, *Br. Assoc. Rep.*, pp. 555–562, Br. Assoc., London.

Rinaldo, A., S. Fagherazzi, S. Lanzoni, M. Marani, and W. E. Dietrich (1999a), Tidal networks: 2. Watershed delineation and comparative network morphology, *Water Resour. Res.*, *35*(12), 3905–3917, doi:10.1029/1999WR900237.

Rinaldo, A., S. Fagherazzi, S. Lanzoni, M. Marani, and W. E. Dietrich (1999b), Tidal networks: 3. Landscape-forming discharges and studies in empirical geomorphic relationships, *Water Resour. Res.*, *35*(12), 3919–3929, doi:10.1029/1999WR900238.

Rinaldo, A., J. R. Banavar, and A. Maritan (2006), Trees, networks, and hydrology, *Water Resour. Res.*, *42*, W06D07, doi:10.1029/2005WR004108.

Rodriguez-Iturbe, I., A. Rinaldo, R. Rigon, R. L. Bras, A. Marani, and E. Ijjasz-Vasquez (1992), Energy dissipation, runoff production, and the three-dimensional structure of river basins, *Water Resour. Res.*, *28*(4), 1095–1103, doi:10.1029/91WR03034.

Roelvink, J. A. (2006), Coastal morphodynamic evolution techniques, *J. Coastal Eng.*, *53*, 177–187.

Roelvink, J. A., T. van Kessel, S. Alfageme, and R. Canizares (2003), Modelling of barrier island response to storms, in *Coastal Sediments 2003 Crossing Disciplinary Boundaries: Proceedings of the International Conference Sheraton Sand Key Resort, Clearwater Beach, Florida, USA 18–23 May 2003*, edited by R. A. Davis, A. Sallenger, and P. Howd, World Sci., Hackensack, N. J.

Savenije, H. H. G. (2001), A simple analytical expression to describe tidal damping or amplification, *J. Hydrol.*, *243*, 205–215, doi:10.1016/S0022-1694(00)00414-5.

Savenije, H. H. G. (2005), *Salinity and Tides in Alluvial Estuaries*, Elsevier, Amsterdam.

Savenije, H. H. G., and E. J. M. Veling (2005), Relation between tidal damping and wave celerity in estuaries, *J. Geophys. Res.*, *110*, C04007, doi:10.1029/2004JC002278.

Schramkowski, G. P., H. M. Schuttelaars, and H. E. De Swart (2002), The effect of geometry and bottom friction on local bed forms in a tidal embayment, *Cont. Shelf Res.*, *22*, 1821–1833, doi:10.1016/S0278-4343(02)00040-7.

Schramkowski, G. P., H. M. Schuttelaars, and H. E. De Swart (2004), Nonlinear channel-shoal dynamics in long tidal embayments, *Ocean Dyn.*, *54*, 399–407, doi:10.1007/s10236-003-0063-6.

Schuttelaars, H. M., and H. E. de Swart (1996), An idealized long-term morphodynamic model of a tidal embayment, *Eur. J. Mech. B*, *15*(1), 55–80.

Schuttelaars, H. M., and H. E. de Swart (1999), Initial formation of channels and shoals in a short tidal embayment, *J. Fluid Mech.*, *386*, 15–42, doi:10.1017/S0022112099004395.

Schuttelaars, H. M., and H. E. de Swart (2000), Multiple morphodynamic equilibria in tidal embayments, *J. Geophys. Res.*, *105*(C10), 24,105–24,118, doi:10.1029/2000JC900110.

Seminara, G., and M. Tubino (2001), Sand bars in tidal channels. part I: Free bars, *J. Fluid Mech.*, *440*, 49–74, doi:10.1017/S0022112001004748.

Singh, V. P., C. T. Yang, and Z.-Q. Deng (2003), Downstream hydraulic geometry relations: 1. Theoretical development, *Water Resour. Res.*, *39*(12), 1337, doi:10.1029/2003WR002484.

Stelling, G. A. (1984), On the construction of computational methods for shallow water flow problems, *Rijkswaterstaat Commun. 35*, Rijkswaterstaat, Hague, Netherlands.

Stelling, G. A. and J. J. Leendertse (1991), Approximation of convective processes B_y cyclic ACI methods, paper presented at 2nd American Society of Civil Engineers Conference on estuarine and coastal modelling, Am. Soc. of Civ. Eng., Tampa, Fla.

Tambroni, N., M. Bolla Pittaluga, and G. Seminara (2005), Laboratory observations of the morphodynamic evolution of tidal channels and tidal inlets, *J. Geophys. Res.*, *110*, F04009, doi:10.1029/2004JF000243.

Toffolon, M., and A. Crosato (2007), Developing macroscale indicators for estuarine morphology: The case of the Scheldt Estuary, *J. Coastal Res.*, *23*(1), 195–212, doi:10.2112/03-0133.1.

Toffolon, M., G. Vignoli, and M. Tubino (2006), Relevant parameters and finite amplitude effects in estuarine hydrodynamics, *J. Geophys. Res.*, *111*, C10014, doi:10.1029/2005JC003104.

Townend, I. H. (1999), Long-term changes in estuary morphology using the entropy method, paper presented at International Association of Hydraulic Engineering and Research Symposium on River, Coastal and Estuarine Morphodynamics, Int. Assoc. of Hydraul. Eng. and Res., Genova, Italy.

Townend, I. H. and R. W. Dun (2000), A diagnostic tool to study long-term changes in estuary morphology, in *Coastal and Estuarine Environments, Sedimentology, Geomorphology and Geoarcheology*, edited by K. Pye and J. R. L. Allen, pp. 75–86, Geol. Soc., London.

Van de Kreeke, J., and K. Robaczewska (1993), Tide induced residual transport of coarse sediment; application to the Ems estuary, *Neth. J. Sea Res.*, *31*(3), 209–220, doi:10.1016/0077-7579(93)90022-K.

van der Spek, A. J. F. (1997), Tidal asymmetry and long-term evolution of holocene tidal basins in the Netherlands: Simulation of palaeo-tides in the Schelde Estuary, *Mar. Geol.*, *141*, 71–90, doi:10.1016/S0025-3227(97)00064-9.

van der Wegen, M., and J. A. Roelvink (2008), Long-term morphodynamic evolution of a tidal embayment using a two-dimensional, process-based model, *J. Geophys. Res.*, *113*, C03016, doi:10.1029/2006JC003983.

van der Wegen, M., D. Q. Thanh, and J. A. Roelvink (2006), Bank erosion and morphodynamic evolution in alluvial estuaries using a process-based 2-D model, paper presented at International Conference on Hydroscience and Engineering Conference 2006, Int. Conf. on Hydrosci. and Eng., Philadelphia, Pa.

van der Wegen, M., Z. B. Wang, H. H. G. Savenije, and J. A. Roelvink (2007), Estuarine evolution using a numerical, process-based approach, paper presented at 5th International Association of Hydraulic Engineering and Research Conference on River, Coastal and Estuarine Morphodynamics, Int. Assoc. of Hydraul. Eng. and Res., Enschede, Netherlands.

van Dongeren, A. D., and H. J. de Vriend (1994), A model of morphological behaviour of tidal basins, *Coastal Eng.*, *22*, 287–310, doi:10.1016/0378-3839(94)90040-X.

van Leeuwen, S. M., and H. E. de Swart (2004), Effect of advective and diffusive sediment transport on the formation of local and global patterns in tidal embayments, *Ocean Dyn.*, *54*, 441–451, doi:10.1007/s10236-004-0092-9.

Van Rijn, L. C. (1993), *Principles of Sediment Transport in Rivers, Estuaries and Coastal Seas*, 535 pp., AQUA, Blokzijl, Netherlands.

Wang, Z. B., C. Jeuken, and H. J. De Vriend (1999), Tidal asymmetry and residual sediment transport in estuaries: A literature study and applications to the Western Scheldt, *WL Delft Hydraul. Rep. Z2749*, WL Delft Hydraul., Delft, Netherlands.

Winterwerp, J. C., Z. B. Wang, M. J. F. Stive, A. Arends, C. Jeuken, C. Kuijper, and P. M. C. Thoolen (2001), A new morphological schematization of the Western Scheldt Estuary, the Netherlands, paper presented at 2nd International Association of Hydraulic Engineering and Research Symposium on River, Coastal and Estuarine Morphodynamics, Int. Assoc. of Hydraul. Eng. and Res., Obihiro, Japan.

Woodroffe, C. D., M. E. Mulrennan, and J. Chappell (1993), Estuarine infill and coastal progradation, southern van Diemen Gulf, northern Australia, *Sediment. Geol.*, *83*, 257–275, doi:10.1016/0037-0738(93)90016-X.

M. van der Wegen and J. A. Roelvink, UNESCO-IHE Institute for Water Education, P.O. Box 3015, NL-2601 DA Delft, Netherlands. (m.vanderwegen@unesco-ihe.org; d.roelvink@unesco-ihe.org)

Z. B. Wang, Deltares, P.O. Box 177, NL-2600 MH Delft, the Netherlands. (zheng.wang@wldelft.nl)

H. H. G. Savenije, Water Resources Section, Civil Engineering and Geosciences Faculty, Delft University of Technology, P.O. Box 5048, NL-2600 GA Delft, Netherlands. (h.h.g.savenije@tudelft.nl)